Statistical Prediction of Laminar-turbulent Transition

Robert Rubinstein and Meelan Choudhari
NASA Langley Research Center, Hampton, Virginia

ICASE
NASA Langley Research Center
Hampton, Virginia

Operated by Universities Space Research Association

National Aeronautics and
Space Administration

Langley Research Center
Hampton, Virginia 23681-2199

December 2000

Form SF298 Citation Data

Report Date ("DD MON YYYY") 00DEC2000	Report Type N/A	Dates Covered (from... to) ("DD MON YYYY")

Title and Subtitle	Contract or Grant Number
Statistical Prediction of Laminar-turbulent Transition	
	Program Element Number

Authors	Project Number
Robert Rubinstein and Meelan Choudhari	
	Task Number
	Work Unit Number

Performing Organization Name(s) and Address(es)	Performing Organization Number(s)
ICASE NASA Langley Research Center Hampton, Virginia	NASA/CR-2000-210632 ICASE Report No. 2000-50

Sponsoring/Monitoring Agency Name(s) and Address(es)	Monitoring Agency Acronym
	Monitoring Agency Report Number(s)

Distribution/Availability Statement
Approved for public release, distribution unlimited

Supplementary Notes

Abstract
Abstract. Stochastic versions of stability equations are considered as a means to develop integrated models of transition and turbulence. Two types of stochastic models are considered: probability density function evolution equations for stability mode amplitudes, and Langevin models based on representative stability theories including the resonant triad model and the parabolized stability equations. The rst type of model can describe the eect of initial phase dierences among disturbance modes on transition location. The second type of model describes the growth of random disturbances as transition proceeds and provides a natural framework in which to couple transition and turbulence models. Coupling of parabolized stability equations with either subgrid stress models or with conventional turbulence models is also discussed as an alternative route to achieve the goal of integrated turbulence and transition modeling.

Subject Terms

Document Classification	Classification of SF298
unclassified	unclassified

Classification of Abstract	Limitation of Abstract
unclassified	unlimited

Number of Pages	
35	

STATISTICAL PREDICTION OF LAMINAR-TURBULENT TRANSITION

ROBERT RUBINSTEIN* AND MEELAN CHOUDHARI†

Abstract. Stochastic versions of stability equations are considered as a means to develop integrated models of transition and turbulence. Two types of stochastic models are considered: probability density function evolution equations for stability mode amplitudes, and Langevin models based on representative stability theories including the resonant triad model and the parabolized stability equations. The first type of model can describe the effect of initial phase differences among disturbance modes on transition location. The second type of model describes the growth of random disturbances as transition proceeds and provides a natural framework in which to couple transition and turbulence models. Coupling of parabolized stability equations with either subgrid stress models or with conventional turbulence models is also discussed as an alternative route to achieve the goal of integrated turbulence and transition modeling.

Key words. turbulence, transition, parabolized stability equations, resonant triads

Subject classification. Fluid Mechanics

1. Introduction. Recent developments in computational fluid dynamics flows have revealed the need for integrated modeling of turbulence and transition. In many external aerodynamic flows, such as the flow past high-lift airfoil configurations, low-pressure turbine blades, and the Mars flyer design proposed by NASA (C. L. Streett, private communication), accurate prediction of crucial bulk parameters like the lift and drag coefficients requires that flow computation be transition sensitized. In high-lift applications in particular, the laminar and turbulent regions are tightly coupled through the dependence of separation and reattachment characteristics on transition location; the predicted flow can vary from fully attached to massively separated depending on the transition location imposed on the flow solver [25]. Recent computations [38] have shown that whereas most turbulence models can predict many external flows with adequate accuracy provided a transition location is specified in advance, no single turbulence model can predict this location in all cases.

A basic obstacle to the integration of turbulence and transition modeling lies in the quite distinct viewpoints of previous research in these fields. Transition studies typically formulate deterministic equations like the Orr-Sommerfeld equation in a wide variety of different problems, whereas turbulence studies apply statistical methods to describe the features common to all turbulent flows. This distinction is best illustrated by comparing the simplest turbulence model, the mixing-length model [49] and the simplest transition prediction scheme, the e^N method [5], [41]. The e^N method is a deterministic procedure based on the linear amplification of the most unstable mode, whereas the mixing-length model appeals to a statistical mechanics analogy to describe the effects of turbulence on the mean flow.

Although these divergent viewpoints arise from the need to describe radically different flow physics, recent developments have tended to bring these fields closer together; thus, recent investigations of bypass transition [33] analyze random initial disturbances, implicitly posing the transition problem statistically. In any case, a synthesis of turbulence and transition modeling is demanded by the need for accurate, seamless computation of transitional flows throughout the entire transition process, from the initial disturbances to

fully developed turbulence.

One approach to integrated modeling of turbulence and transition is to apply low Reynolds number turbulence models directly to transitional flows [1], [7], [11]; this approach treats transition as a special kind of 'non-equilibrium' turbulence. Another general approach is to sensitize existing turbulence models to transition, often by introducing a new field quantity like intermittency [45], [26], [40]. An entirely new approach which treats transition beginning from turbulence modeling is given in [46]. Certainly, models of this type will play a valuable role in the aerodynamic design process. However, due to the limited transition physics embedded in such models, typically through curve fits and/or *ad hoc* calibration against a relatively sparse measurement database, they are not likely to explain potential anamolies in measured aerodynamic performance or yield reliable answers when extrapolation to completely new flow situations (e.g., the Mars flyer application) is required.

In broad terms, the present work is motivated by the desire to retain as much of the transition physics revealed by recent advances in understanding of the transition process reviewed, for example by [16], [22], [14], and [27], yet allow for integrated aerodynamic predictions in a realistic setting. To that end, the current investigation begins with transition and has the ultimate goal of incorporating turbulence prediction in a seamless fashion. Given this overall goal, two main areas present themselves as candidates for further work. The first of these areas concerns the prediction of transition in isolation from the turbulent flow computation, whereas the second area of need is related to the mechanics of coupling the transition prediction with the computation of the turbulent flowfield.

First, let us consider the prediction of transition itself. As noted by Reshotko [34], laminar-turbulent transition in a convectively unstable boundary layer corresponds to the forced response of a rather complex oscillator, namely the laminar basic state. Under the relatively benign disturbance environments that are typical of external aerodynamic flight, the above response may be decomposed into three broad stages: excitation of linearly unstable eigenmodes of the oscillator due to forcing from the external disturbances (i.e., the process of receptivity), initially exponential growth of these eigenmodes as they propagate downstream, and the variety of nonlinear interactions which ensue after the eigenmodes have achieved sufficiently large amplitudes and which eventually lead to turbulence. Any attempt to model the transition process on a rational basis must account for all three stages of the 'oscillator' response.

The current engineering methods for transition prediction typically involve the linear propagation phase alone, with little or no account of receptivity (which initiates transition) or the nonlinear interactions (which actually cause the onset of transition). In spite of their success in predicting transition in a wide range of flows, these N-factor methods lack the physical basis necessary to explain the effects of surface roughness and free-stream unsteadiness, which may be particularly significant in flows such as swept wing boundary layers and high-lift flows. Thus, as an essential aspect of integrated modeling of transition and turbulence, it is necessary to develop rational prediction methods that couple the various stages of transition itself. A preliminary attempt along these lines, which focused on a controlled disturbance environment involving sinusoidal surface waviness and a monochromatic acoustic disturbance, was presented in [3]. However, considerable advancement is necessary to enable similar predictions in a realistic setting.

In view of the complexity of the forcing fields encountered in practical applications, integrated transition prediction needs to be performed within a stochastic framework that is capable of analyzing the effects of randomness and uncertainties in the flow environment. The concept of stochastic transition prediction represents a major theme behind the work reported in this paper. The objective here is not so much to develop and present a well-tested recipe towards this goal, but to outline the various issues introduced by

stochasticity, explore potential ways in which they might be addressed, and examine the potential merits and demerits of each approach. Although mainly aimed at integrated transition and turbulence modeling, we note that such work would also be relevant to developing stochastic control schemes for laminar-turbulent transition.

In principle, statistical consideration of the forced-oscillator response should include the uncertainties associated with both oscillator characteristics (i.e., undisturbed laminar state) and the forcing environment. Of these two, the stochastic character of the forcing is perhaps more important, and is what is emphasized here. In general terms, we consider how deterministic models for a given stage of the transition process (which may be considered as well-established at this point) may be extended to a stochastic setting by treating the input conditions as random rather than fully specified.

In this paper, we assume that the dominant receptivity occurs through linear mechanisms and hence the overall problem of stochastic disturbance evolution in a boundary layer may be decomposed into two separate problems: the receptivity problem that predicts the statistics of initial disturbances (i.e., instability modes) as functions of input forcing, and the propagation stage which predicts how these statistical characteristics evolve as the instability waves amplify and eventually interact through nonlinear mechanisms. Given the system parameters (i.e., a plant model), the response of a linear, deterministic system to stochastic input can be predicted rather simply since the second moments of the response are directly proportional to those of the input, with the scaling factor begin the known (deterministic) transfer function. Thus, it is relatively straightforward to extend the available models for receptivity and linear growth to a stochastic setting. Accordingly, we focus our attention on stochastic aspects of the nonlinear propagation phase, for which there is no unique transfer function as the latter now becomes a function of the input parameters (i.e., initial amplitude spectrum).

As transition progresses, a sequence of secondary and higher order instabilities are excited leading to the emergence of smaller scales of motion; with continued excitation of small scales, memory of the details of the original state fades, and gradually a statistically steady state of turbulence is reached. Two points are worth noting in this context. First, as the system becomes chaotic during the laminar breakdown stage, stochastic modeling is necessary even if there were no uncertainties in the forcing environment. Second, stochastic formulation of the transition models provides a natural link between transition theory and turbulence modeling. Of course, passing from a deterministic to a stochastic transition analysis is not trivial, particularly in view of nonlinearity of the problem. The details of the path to turbulence, in which different modes are significant during different phases in the evolution, is highly case dependent. Therefore, a direct simulation of the stochastic problem, which would require simulating a large number of these paths, is impractical. This problem is much more severe than the problem of simulating fully developed turbulence, in which ergodicity helps permit the evaluation of statistics. The present paper represents but a first step to a statistical model of transition.

An outline of the paper is as follows. To begin, we briefly review the theory of receptivity, since in many external flows, receptivity analysis will determine the initial disturbance spectrum. Following [8], we emphasize the stochastic aspects of the problem, namely the connection between the random free-stream disturbances and roughness distributions and the probability density function of the phase and amplitude of the generated Tollmien-Schlichting waves.

The subsequent evolution of the generated instability waves (particularly, during the nonlinear stage) is examined next. On a determinstic level, the disturbance evolution problem can be addressed using models of varying degrees of sophistication and accuracy including Craik's model for resonant triads of Tollmien-

Schlichting waves [12], rational high Reynolds number asymptotics [14], parabolized stability equations [4], large eddy simulation [18], and direct numerical simulation [33],[51]. To achieve the goal of integrated transition and turbulence modeling, we start by applying these models in a stochastic setting, treating the initial disturbance spectrum as random rather than deterministic. We begin by considering the simplest model for nonlinear disturbance interactions, namely Craik's model [12], which provides a simplified account of nonlinear interactions via a viscous critical layer. Despite its shortcomings from the viewpoint of systematic asymptotics [14], this model has been shown to yield predictions which agree reasonably well with many experimental observations [20]. In the present context, it provides a simple model to illustrate the combined effects of nonlinearity and randomness on the propagation of instability waves. Moreover, by connecting the amplification of subharmonics to the growth of phase coherence, this model suggests a link between transition and turbulence, where the growth of phase coherence is closely connected to energy transfer. Fully developed turbulent flow exists because of a balance between triad interactions, which promote phase coherence, and coupling to all other modes which destroys it [23]. The resonant triad model can be understood from this viewpoint as the first phase in establishing this balance.

We next outline the extension of the resonant triad model to more complex interactions. Specifically, we examine the interactions between more than three instability waves, nonlinear effects in a non-equilibrium critical layer, and predictions for the strongly nonlinear regime. These extensions raise the important issue of modeling the effects of higher order modes which have not been explicitly resolved by the model being considered. The model which seems best suited for engineering predictions of transition and could potentially extend into the strongly nonlinear regime is the parabolized stability equations (PSE) [16]. A preliminary discussion is given concerning how PSE can be treated in a stochastic setting.

Finally, we describe our proposal for a general, integrated turbulence and transition model: a generalized PSE restricted to a relatively small number of modes with the effect of the remaining modes accounted for through modified damping and random forcing. The crux of our proposal is that turbulence effects can also be included in the model the same way. Such a model would be a compromise between transition-sensitized Reynolds-averaged Navier-Stokes (RANS) and large eddy simulation (LES) or direct numerical simulation (DNS).

2. Stochastic aspects of the disturbance generation and evolution through the weakly non-linear stage.

2.1. Summary of the receptivity problem. The statistical analysis of transition in a convectively unstable flow begins with the random initial conditions, which, barring uncertainties or inaccuracies in the mean flow prediction, are the only source of randomness in the problem. In the Goldstein-Ruban-Zavol'skii theory [15], [36], [52], receptivity is analyzed as the excitation of a free Tollmien-Schlichting wave through the interaction between a specified ambient unsteady disturbance with surface roughness of known shape and size. Provided that the wavenumber spectrum of the surface roughness and the characteristic frequency of the ambient disturbance overlap respectively the wavelength and frequency of a free Tollmien-Schlichting wave, in low-speed flows, this wave can be excited and subsequently amplified.

Receptivity analysis is most often formulated as a deterministic problem. Although some stochastic aspects have been explored in [8], this analysis was limited to evaluating the rms amplitude of the instability wave. By averaging over the roughness distribution, phase information is lost, and only averages remain. This work has been extended to transient analysis of receptivity by formulating the problem as a stochastic differential equation. The result is a description of the growth of receptivity amplitudes by means of a Fokker-Planck equation [37]. The conclusion from this work for the present purpose is simply this: because

receptivity is a linear problem, if the phases in the disturbance environment are random, then the phases in the initial random distribution of Tollmien- Schlichting waves will also be random.

While randomness of the phase has no influence on the linear evolution of the instability waves, there exist cases in which the disturbance phase can have a significant impact on the nonlinear evolution as illustrated later in this section.

2.2. Resonant triad evolution in a boundary layer. The defects of deterministic transition predictions based on linear amplification alone are well-known: the analysis cannot account for the rapid onset of three-dimensional behavior as transition is approached, or for the mean-flow modification due to the disturbance growth. This is because both of these features are due to disturbance nonlinearity and the neglect of nonlinear effects on disturbance evolution eventually invalidates the theory. In the following subsections, we illustrate the dependence of disturbance evolution on the relative initial phase of different instability modes in the simplest context to set the stage for a stochastic analysis of nonlinear disturbance evolution.

Many weakly nonlinear analyses have been introduced in transition theory to explain the onset of three-dimensional behavior. We consider the simplest theory of this type, namely Craik's theory [12] of resonant interaction between a triad of Tollmien-Schlichting waves which shows how oblique subharmonics can be amplified, even if they are linearly damped.

2.2.1. Craik's model: deterministic triad interaction problem. The analysis [12] begins with a primary, two-dimensional Tollmien-Schlichting wave in a two-dimensional parallel mean flow

$$(2.1) \qquad \Psi_3 = Re\{A_3\phi_3(y)e^{i[\alpha x - \omega t]}\}$$

which, together with a pair of resonant subharmonics,

$$(2.2) \qquad \Psi_{1,2} = Re\{A_{1,2}\phi_{1,2}(y)e^{i[(\alpha/2)x \pm \beta z - (\omega/2)t]}\}$$

represents a special case of a resonant triad of waves. Here, x, y, z denote the streamwise, normal, and the spanwise directions respectively; t denotes time, α, β, and ω denote the disturbance wavenumber and frequency for a given mode, ϕ_i ($i = 1, 2, 3$) denote the appropriately normalized eigenfunctions. The disturbance amplitudes A_i ($i = 1, 2, 3$) are slowly varying functions of space,

$$(2.3) \qquad A_i = A_i(x) \quad \text{with} \mid \frac{1}{A_i}\frac{\partial A_i}{\partial x} \mid \ll \alpha$$

or of time,

$$(2.4) \qquad A_i = A_i(t) \quad \text{with} \mid \frac{1}{A_i}\frac{\partial A_i}{\partial t} \mid \ll \omega$$

depending on whether the disturbance evolves in space x or time t. The latter distinction is perhaps unimportant for this paper. However, to facilitate comparison with previous deterministic analyses, we will treat only the spatial case herein.

Under the parallel-flow assumption, Craik's heuristic analysis led to the following set of ordinary differential equations for the (complex) amplitudes of the resonant triad of waves defined in Eqs. (2.1) and (2.2):

$$
\begin{aligned}
\dot{b}_1 &= \tilde{\sigma} b_1 + b_3 b_2^* \\
\dot{b}_2 &= \tilde{\sigma} b_2 + b_3 b_1^* \\
(2.5) \qquad \dot{b}_3 &= \sigma b_3 + e^{i\phi} b_1 b_2
\end{aligned}
$$

5

where b_i, $(i = 1, 2, 3)$ denote normalized forms of the complex amplitudes A_i and the dot denotes differentiation along the evolution coordinate (i.e. x for the spatial disturbance evolution considered here). In Eq. (2.5), $\tilde{\sigma}$ and σ are the normalized linear growth rates of the subharmonic and primary waves respectively, and the angle ϕ models the effect of detuning between the primary and subharmonics. Eq. (2.5) applies only in the parallel-flow limit, in which the nonlinear growth is assumed to occur on a scale that is much smaller than the scale of the mean boundary layer growth (i.e. nonparallel scale). Eq. (2.5) also applies more generally to problems in which the growth rates become weak functions of x through small effects of non-parallism. This generalization will be used in a subsequent case study.

An important simplification of Eqs. (2.5) is provided by the equations for *parametric excitation*:

$$\dot{b}_1 = \tilde{\sigma} b_1 + b_3 b_2^*$$
$$\dot{b}_2 = \tilde{\sigma} b_2 + b_3 b_1^*$$
(2.6)
$$\dot{b}_3 = \sigma b_3$$

wherein the nonlinear term in the equation for the primary amplitude b_3 has been dropped, hence b_3 undergoes purely linear growth. This limiting case corresponds to the parametric region $|b_1|, |b_2| \ll |b_3|$ which is typical of the initial phase of nonlinear growth.

In terms of amplitude-phase variables defined by

(2.7)
$$b_i = r_i e^{i\theta_i},$$

Eq. (2.5) becomes

$$\dot{r}_1 = r_2 r_3 \cos\theta + \tilde{\sigma} r_1$$
$$\dot{r}_2 = r_1 r_3 \cos\theta + \tilde{\sigma} r_2$$
$$\dot{r}_3 = r_1 r_2 \cos(\phi - \theta) + \sigma r_3$$
(2.8)
$$\dot{\theta} = \frac{r_1 r_2}{r_3} \sin(\phi - \theta) - \frac{r_1 r_3}{r_2} \sin\theta - \frac{r_2 r_3}{r_1} \sin\theta$$

Observe that the amplitude evolution depends, not on the individual phases θ_i, but only on the single phase variable

(2.9)
$$\theta = \theta_1 + \theta_2 - \theta_3$$

Many special solutions and properties of the triad equations can be derived [12], [48]; however, for the purposes of transition studies, a simple generic picture is adequate. In general, the subharmonics are amplified, eventually overtaking the primary. During growth, the amplitudes of the subharmonics become equal $(r_1 = r_2 = r)$ and a condition of phase-locking $(\theta = 0)$ develops. After the onset of phase-locking, the solution undergoes explosive growth, leading to a finite-time singularity of the solution [48]. Amplification can occur even if the subharmonics are linearly stable $(\tilde{\sigma} < 0)$, and also even if the primary is linearly stable $(\sigma < 0)$ [30].

This behavior is immediately apparent from the closed-form solution for the case of parametric excitation Eq. (2.6):

$$b_1(t) = \frac{1}{2}[b_1(0) + b_2(0)^*]e^{(e^{\sigma t} - 1)/\sigma + \tilde{\sigma} t} + \frac{1}{2}[b_1(0) - b_2(0)^*]e^{-(e^{\sigma t} - 1)/\sigma + \tilde{\sigma} t}$$
(2.10)
$$b_2(t) = \frac{1}{2}[b_1(0)^* + b_2(0)]e^{(e^{\sigma t} - 1)/\sigma + \tilde{\sigma} t} - \frac{1}{2}[b_1(0)^* - b_2(0)]e^{-(e^{\sigma t} - 1)/\sigma + \tilde{\sigma} t}$$

which shows that the subharmonics can amplify exponentially even if $\tilde{\sigma} = 0$. Eq. (2.10) illustrates the two features noted above: at sufficiently long time, amplitudes of the two subharmonics become equal (i.e. $\mid b_1 \mid = \mid b_2 \mid$), and $b_1 b_2$ becomes real so that θ approaches zero.

The parametric excitation case also reveals that amplification is phase-dependent: if $b_2(0) = -b_1(0)$ is real, so that the initial phase $\theta(0) = \pi$, then the growing double exponential term does not occur and we have

$$b_1(t) = b_1(0)e^{-(e^{\sigma t}-1)/\sigma+\tilde{\sigma}t}$$

(2.11)
$$b_2(t) = -b_1(0)e^{-(e^{\sigma t}-1)/\sigma+\tilde{\sigma}t}.$$

In this case, the subharmonics will actually decay in the absence of linear growth.

We note that the dependence of subharmonic amplification on its phase relative to the primary wave is well-known in the context of mixing-layer instabilities [30]. Analogous behavior in wall-bounded flows, albeit not equally emphasized in the literature, has been measured [39] and theoretically predicted [53]. Unfortunately however, the effects of initial phase lag on transition location have not been explored in detail as yet. A preliminary attempt using admittedly crude modeling is made below (see Fig. 2.8). Further examination using both nonlinear PSE and wind tunnel experiments is planned for the near future.

The general features of triad evolution are depicted in Fig. 2.1 which were obtained from numerical integration of Eqs. (2.5) using a fourth-order Runge-Kutta method starting from initial values of the phase $\theta(0) = N\pi/4, N = 1, \cdots 16$. In all cases, initial amplitudes were held fixed at $r_1(0) = r_2(0) = 0.1, r_3(0) = 1.0$ with initial growth rates $\tilde{\sigma} = 0$. (i.e. linearly neutral subharmonics), and $\sigma = 0.1$. Figure 2.1 shows both the evolution of the phase, in which "locking" is clearly evident, and the evolution of the primary and subharmonic amplitudes; a strong connection between subharmonic amplification and phase locking is suggested by a comparison between the phase and amplitude evolution.
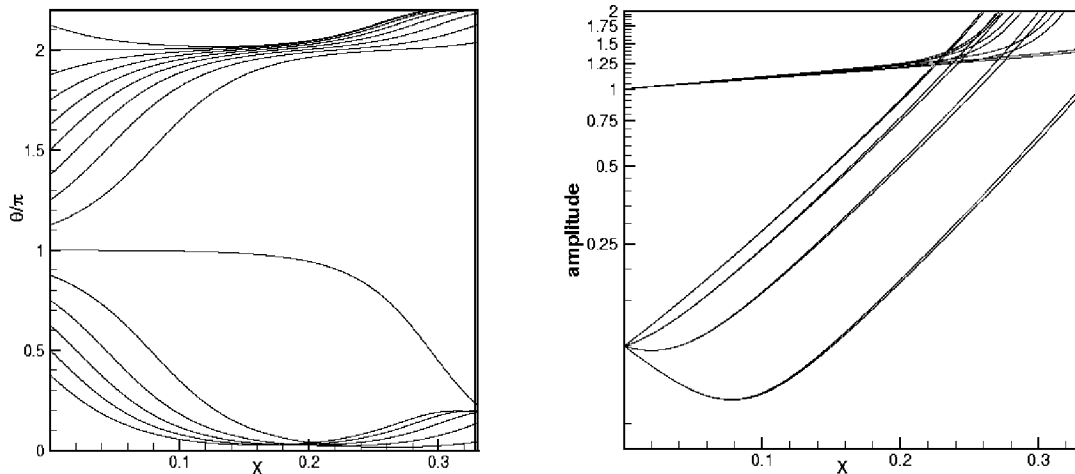

FIG. 2.1. *Effect of initial phase on subharmonic amplification in the nonlinear evolution of a resonant triad. The downstream development of the phase variable θ and of the primary and subharmonic amplitudes are shown for variable initial θ. Parameters in Eq. (2.5) are: $\sigma = 0.1$ and $\tilde{\sigma} = 0$; the dephasing factor $\phi = 0$. Initial conditions are: primary amplitude $r_3(0) = 1.0$ and subharmonic amplitudes $r_1(0) = r_2(0) = 0.1$. The initial phase $\theta(0)$ is uniformly distributed from $-\pi$ to π. The governing equations are fully nonlinear triad interactions, Eq. (2.5).*

Observe that even though the triad system Eq. (2.5) supports an equilibrium solution of the form $\theta = \pi$, that solution is unstable, with the only long-time attractor being the phase-locked solution $\theta = 0$ as observed earlier by [14] in a similar context using high Reynolds number asymptotic theory.

Fig. 2.2 shows the same calculation for the linear theory of parametric excitation. The picture is naturally considerably simpler since the primary only undergoes linear growth. The curve with $\theta(0) = \pi$ maintains its initial value througout. Therefore, unlike the fully coupled case illustrated by Fig. 2.1, the subharmonic amplitude in this case continues to decay during its evolution.
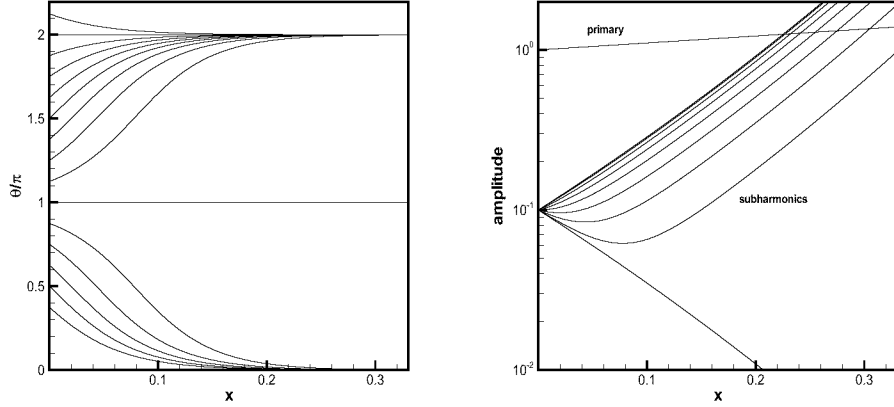

FIG. 2.2. *Effect of initial phase on subharmonic amplification in the case of parametric excitation. Disturbance parameters and initial conditions are as in Fig. 2.1.*

2.2.2. Stochastic formulation of triad evolution: probability density function approach.

The analysis of subharmonic growth suggests a role for a statistical theory of resonant interactions. Since the growth of subharmonic disturbances depends on their initial phase, an exact description will require a knowledge of the initial phase; but if these initial conditions are referred to a receptivity calculation, then as Sect. 2.1 suggests, even if the initial disturbance amplitudes were known with relative precision, the initial phase distribution could not be established in general. Thus, the initial conditions for the theory of subharmonic growth are best described by a probability density function (PDF) for initial amplitudes and phases. From this viewpoint, the best description of subharmonic growth is given by the evolution of this PDF.

For the sake of brevity, we formulate the evolution equation for the case of equal subharmonic amplitudes, $r_1 = r_2 = r$. This condition is preserved by the equations of motion, and as noted previously, the system eventually evolves to this condition in any case. Applying standard methods [31], one finds that the joint probability density $P(r, r_3, \theta; t)$ of amplitudes r, r_3 and the phase variable θ satisfies the first order partial differential equation

$$(2.12) \qquad \frac{\partial P}{\partial t} + \frac{\partial}{\partial r}(F_r P) + \frac{\partial}{\partial r_3}(F_3 P) + \frac{\partial}{\partial \theta}(F_\theta P) = 0$$

where

$$F_r = r r_3 \cos\theta + \tilde{\sigma} r$$
$$F_3 = r^2 \cos(\phi - \theta) + \sigma r_3$$

8

$$(2.13) \qquad F_\theta = \frac{r^2}{r_3} \sin(\phi - \theta) - 2r_3 \sin \theta.$$

Closed equations for the moments of P cannot be obtained, since moments of any given order are found to depend on moments of higher order.

The initial PDF is taken to be independent Gaussian distributions for amplitudes, and initially uniformly distributed phase,

$$(2.14) \qquad P(r, r_3, \theta; 0) = \frac{1}{2\pi} N(r \mid r_0, \sigma_0) N(r_3 \mid r_{3,0}, \sigma_3)$$

where

$$(2.15) \qquad N(x \mid x_0, \sigma) = \frac{1}{\sqrt{2\pi\sigma^2}} e^{-(x-x_0)^2/2\sigma^2}.$$

Since Eq. (2.12) is a linear first-order partial differential equation in a conservative form, numerical integration is straightforward. The method used for solving this equation numerically is described in detail in Appendix I. The numerical integration reproduced the qualitative features of the deterministic analysis as described earlier via Figs. 2.1 and 2.2. The marginal probability densities for subharmonic amplitude and phase,

$$
\begin{aligned}
P(r_3, t) &= \int_0^\infty dr \int_0^{2\pi} d\theta \; P(r, r_3, \theta; t) \\
P(\theta, t) &= \int_0^\infty dr \int_0^\infty dr_3 \; P(r, r_3, \theta; t)
\end{aligned}
$$
(2.16)

are shown for the case of parametric excitation in Fig. 2.3.

This case is chosen for preliminary code verification because the primary amplitude probability density must be constant as a function of the centered normalized variable $\gamma = (r - \langle r \rangle)/\sigma$. The primary amplitude PDF remains Gaussian and unchanged after this normalization. Fig. 2.3 shows that the subharmonic amplitude becomes bimodal as time increases. The bimodality arises because paths exist for which the subharmonic amplitude decays at first. This M-shaped PDF can be compared with the measurements of [29] in the analogous case of a transitioning mixing layer. Fig. 2.3 also presents another picture of the strong tendency to phase locking.

For quantitative validation of the method, we compare the results with some partially analytic results available for the case of parametric excitation. A straighforward calculation shows that the distribution of phase is related to the initially uniform distribution ψ through the equation

$$(2.17) \qquad d\theta = -2R \frac{1 - \cos \psi}{\sin^2 \psi + (\cos \psi - 1)^2 R^2} d\psi$$

where ψ is uniformly distributed, and the factor R is the double exponential of Eq. (2.10), i.e.,

$$(2.18) \qquad R = \exp[\frac{1}{\sigma} \exp(\sigma t - 1) + \bar{\sigma} t].$$

The marginal probability density function of the phase is compared with the exact result in Fig. 2.4 . The agreement is satisfactory. Analytical expressions for the amplitude PDF's cannot be derived; however, the mean and variance of the primary and subharmonic are easily evaluated numerically in this case. The results are compared with the predictions of the PDF code in Fig. 2.4. The agreement is satisfactory except that the predictions of the subharmonic standard deviation become inaccurate near the end of the simulation. This inaccuracy may reflect the low order accuracy of the finite volume algorithm used in the code.
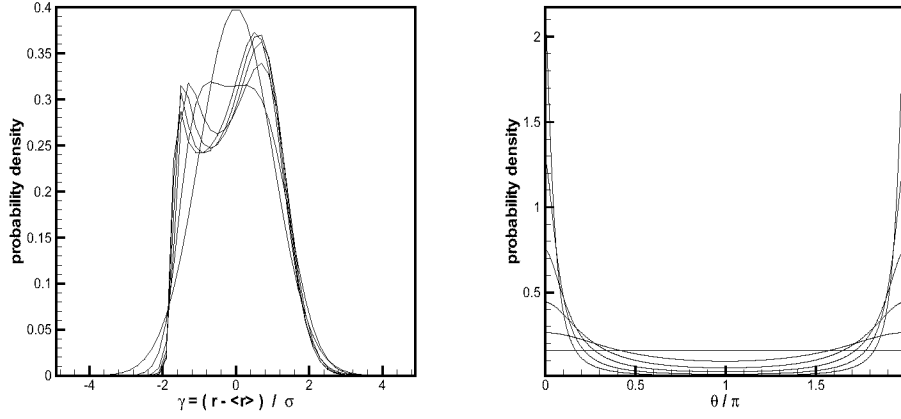
FIG. 2.3. *Subharmonic amplitude and phase PDF's for different Re under parametric excitation. Initial phase is uniformly distributed from $-\pi$ to π; initial primary amplitude is Gaussian with mean 1 and standard deviation 0.1, and equal initial subharmonic amplitudes are Gaussian with mean 0.1 and standard deviation 0.01. Disturbance parameters $\sigma, \tilde{\sigma}, \phi$ are as in Fig. 2.1. As Re increases, the initially Gaussian subharmonic amplitude PDF becomes bimodal and the initially uniform phase PDF becomes concentrated at $\theta = 0$.*
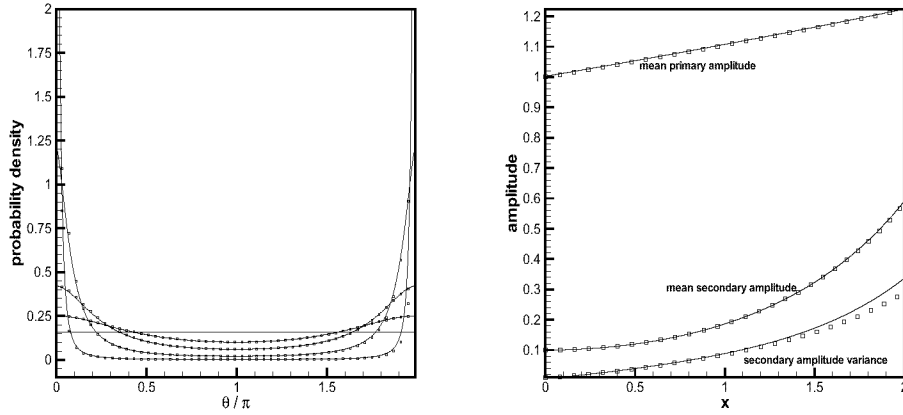

FIG. 2.4. *Validation of numerical solution of joint PDF evolution equation for parametric excitation case: initial conditions are as in Fig. 2.3. Left - comparison between exact (dots) phase evolution and numerical solution (lines) of joint PDF equation. Right - comparison between exact (symbols) and computed (lines) amplitude statistics. Disturbance parameters $\sigma, \tilde{\sigma}, \phi$ are as in Fig. 2.1.*

2.3. Stochastic form of triad evolution: particle method. Although direct solution of the PDF evolution equation Eq. (2.12) is feasible, the computation time required is excessive. Even with the assumption that the amplitudes of the two subharmonic modes are equal, integration up to the time that the subharmonics exceed the primary required several days on a workstation. As noted in Ref. [31], the main difficulty in integrating any PDF evolution equation is dimensionality: updating a PDF with d variables with N degrees of freedom each requires about N^d operations per time step.

The *particle method* of Pope [31] mitigates this difficulty at the expense of a coarser description of the PDF. In the present problem, the particle method can be formulated as follows. Consider the general

problem with independent amplitudes r_1, r_2, r_3. Replace the initial PDF by a sum of delta functions,

$$P(r_1, r_2, r_3, \theta; 0) \approx \sum_{n_1, n_2, n_3, n_\theta} P(n_1, n_2, n_3, n_\theta) \times$$

(2.19)
$$\delta(r_1 - r_{n_1})\delta(r_2 - r_{n_2})\delta(r_3 - r_{n_3})\delta(\theta - \theta_{n_\theta})$$

where the points $r_{n_i}, \theta_{n_\theta}$ at which the PDF is sampled are arbitrary, but deterministic. These points could be chosen based on a Gaussian quadrature scheme, for example. Note that if the variables r_i, θ are assumed to be independent initially, then

(2.20)
$$P(n_1, n_2, n_3, n_\theta) = P(n_1)P(n_2)P(n_3)P(\theta)$$

Next, the deterministic evolution equations are integrated for an ensemble of initial conditions $r_1(0) = r_{n_1}, r_2(0) = r_{n_2}, r_3(0) = r_{n_3}, \theta(0) = \theta_{n_\theta}$. The PDF at time t is approximated by the discrete sum

$$P(r_1, r_2, r_3, \theta; t) \approx \sum_{n_1, n_2, n_3, n_\theta} P(n_1, n_2, n_3, n_\theta) \times$$

(2.21)
$$\delta(r_1 - r_{n_1}(t))\delta(r_2 - r_{n_2}(t))\delta(r_3 - r_{n_3}(t))\delta(\theta - \theta_{n_\theta}(t)).$$

This scheme is not a Monte Carlo method, because the initial PDF is not sampled randomly; instead, the sampling is deterministic but weighted according to the specified initial PDF. An important feature of the method, which is evident from Eq. (2.21), is that it conserves total probability.

To assess the accuracy of this particle method, the statistics shown in Fig. 2.4 were recomputed and compared with the exact results in Fig. 2.5. Evidently, the agreement is much more satisfactory.
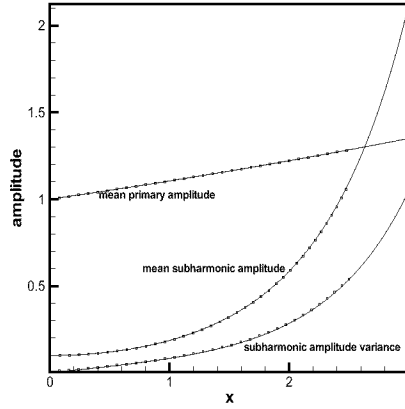

FIG. 2.5. *Comparison between theoretical and computed amplitude statistics for parametric excitation: lines - computation (particle method), symbols - theory. Initial conditions and disturbance parameters $\sigma, \tilde{\sigma}, \phi$ are as in Fig. 2.1.*

One must note, however, that one of the advantages of the probability density function approach is that it is robust with respect to any finite-time singularities observed in individual solutions of the deterministic evolution equations. The particle method, on the other hand, requires one to remove any trajectories that approach a singularity (and to account for this removal in some reasonable manner). However, this is not necessarily a significant limitation as the singularities indicate limitations of the underlying (deterministic) model and, hence, are either delayed or bypassed altogether in a real application after the model is suitably generalized to include the relevant physics neglected previously.

2.4. Stochastic triad evolution: case study and comparison with experiment. The particle method was applied to examine stochastic aspects of the triad evolution in a flat-plate boundary layer. In particular, the case of a symmetric resonant triad which had previously been examined in Ref. [53] in a deterministic setting was considered. This triad was comprised of a two-dimensional fundamental wave with a dimensionless frequency $F = 115 \times 10^{-6}$ and its subharmonics with a spanwise wavenumber given by $\beta/Re = 0.22 \times 10^{-6}$. (For a definition of these dimensionless parameters, the reader is refered to [53].)

To allow for the effects of the growth of the mean boundary layer, as well as the effects of small detuning, the triad equation set Eq. (2.5) was replaced by the slightly more general system

$$\dot{b}_1 = \tilde{\sigma}(x)b_1 + S_{1,23}(x)b_2^*b_3$$
$$\dot{b}_2 = \tilde{\sigma}(x)b_2 + S_{2,13}(x)b_1^*b_3$$
(2.22)
$$\dot{b}_3 = \sigma(x)b_3 + S_{3,12}(x)b_1 b_2$$

where the x dependence of the linear growth rates σ and $\tilde{\sigma}$ and the nonlinear interaction coefficients reflect the effects of weak mean-flow non-parallelism. The interaction coefficients $S_{l,jk}$ can be complex to allow for detuning effects. The evolution variable is streamwise distance, measured in this case as a downstream Reynolds number. This system can also be written in terms of amplitude and phase variables as

$$\dot{r}_1 = \tilde{\sigma}r_1 + R_{1,23}(x)r_2r_3 \cos(\theta + \phi_1(x))$$
$$\dot{r}_2 = \tilde{\sigma}r_2 + R_{2,31}(x)r_2r_1 \cos(\theta + \phi_2(x))$$
$$\dot{r}_3 = \sigma r_3 + R_{3,12}(x)r_1r_2 \cos(\phi_3(x) - \theta)$$
(2.23) $$\dot{\theta} = R_{3,12}\frac{r_1r_2}{r_3}\sin(\phi_3(x) - \theta) - R_{2,31}\frac{r_1r_3}{r_2}\sin(\theta + \phi_2(x)) - R_{1,23}\frac{r_2r_3}{r_1}\sin(\theta + \phi_1(x))$$

where we have set

(2.24) $$S_{i,jk} = R_{i,jk}e^{i\phi_i}.$$

The values of the nonlinear coefficients $S_{i,jk}$ as functions of the Reynolds number were based on Table 1 of [53]. The initial PDF is given in Eq. (2.14).

The results are shown in Fig. 2.6. The right-hand graph can be compared with Fig. 2 of [53]. The subharmonic amplitudes are initially unequal; however, the tendency of these amplitudes to equalize is evident. The subharmonics overtake the primary at a Reynolds number of about 700., in agreement with the analysis of [53]. After this point, the entire system undergoes explosive growth leading to a singularity in all three amplitudes. The left-hand graph shows the corresponding phase evolution. Both the close connection between the development of phase locking and the onset of explosive nonlinear growth and the effect of initial phase on subharmonic growth which were observed in the previous model problems also exist in this more realistic example.

In order to illustrate the connection between subharmonic amplification and transition, the conditions analyzed in [53] were modified slightly. In Fig. 2.7, the initial amplitudes of the two subharmonics are one-half the initial primary amplitude. Initial standard deviations of the amplitudes are set at ten percent of the mean. The effect of initial phase difference on subharmonic growth is considerably enhanced by this change of initial amplitude.

To connect this analysis to transition, Fig. 2.8 shows the probability that the subharmonic amplitude exceeds the local primary amplitude. Although the crossover location is not the same as the transition onset location (which cannot be predicted within the limited framework of resonant triad interaction), it
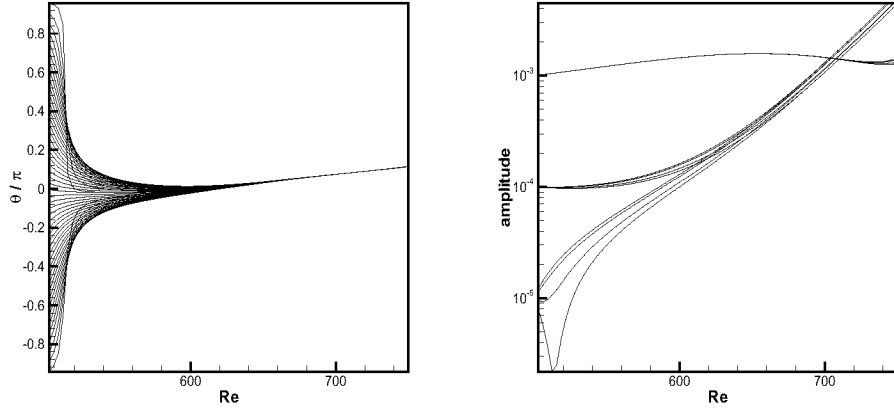
FIG. 2.6. *Phase locking and subharmonic amplitude equalization during triad evolution in the problem analyzed in Ref. [53]. Left - phase evolution as a function of Reynolds number. Right - amplitudes of primary and subharmonics as functions of Reynolds number. The right-hand figure can be compared with Fig. 2 of Ref. [53].*
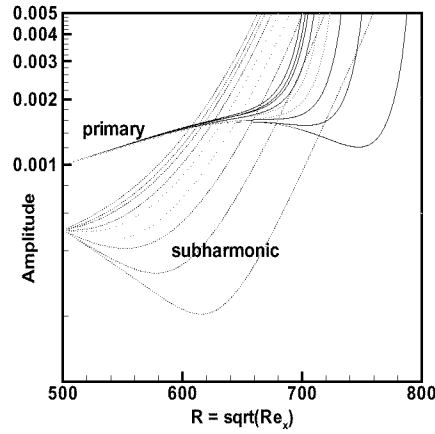
FIG. 2.7. *Effect of initial phase on triad evolution. Primary and subharmonic amplitudes are shown as functions of local Reynolds number. All triad evolution parameters are based on Fig. 2 of Ref. [53], except that the initial subharmonic amplitudes are both equal to 0.5 times the initial primary amplitude.*

does harbinger the potential onset of stronger nonlinear interactions and, hence, the approach of transition (assuming, of course, that the primary amplitude involved is significantly large as well).

With a suitable generalization of the underlying model, then, a stochastic transition theory will indicate the probabilistic spread in transition location as a function of uncertainties in the initial disturbance characteristics. In that spirit, Fig. 2.8 may be viewed as a measure of variation in transition onset probability with downstream location.

A qualitative comparison with experimental results [39] is shown in Fig. 2.9. Here, the subharmonic amplitude at selected downstream locations is plotted as a function of initial phase difference between the primary and subharmonic waves.

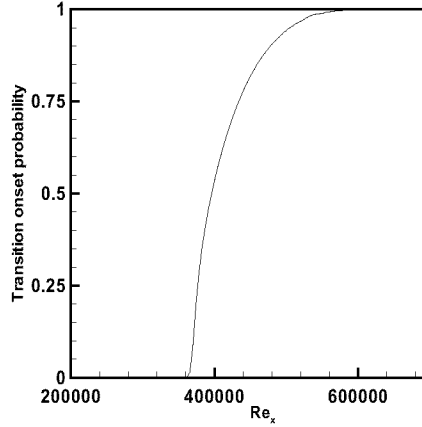FIG. 2.8. *Transition onset probability based on subharmonic growth as function of local Reynolds number. The conditions analyzed are the same as in Fig. 2.7. Transition onset is assumed to occur when the primary and subharmonic amplitudes are equal. The spread in transition onset location is due to uncertainty of the initial phase and amplitude.*
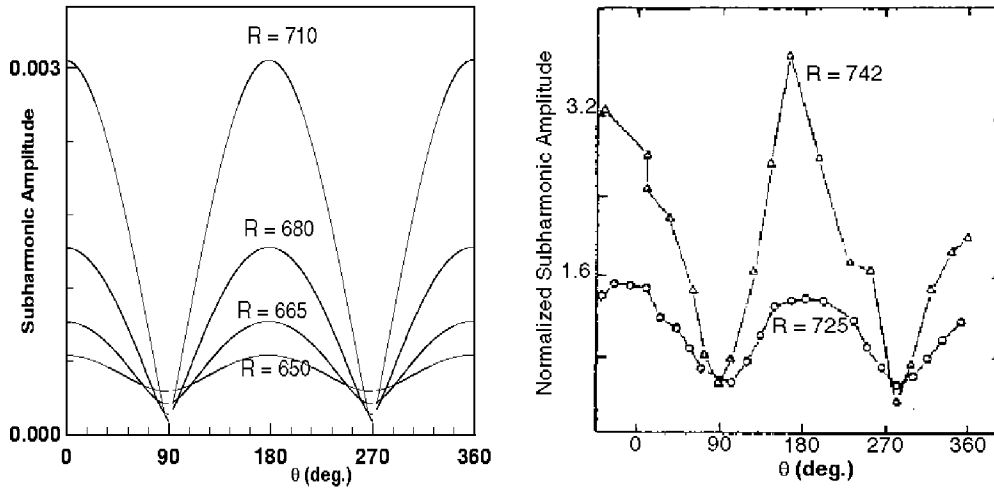
FIG. 2.9. *Subharmonic amplitude as a function of initial phase difference between subharmonic and primary modes: left - theory, right - experiment of [39]. The triad parameters are somewhat different, therefore the comparison is qualitative.*

3. Extension of stochastic formulation to more general nonlinear disturbance evolution models.

By accounting for the rapid onset of three-dimensionality in transitional flows, the resonant triad model overcomes one of the important limitations of linear stability theory; this was actually one of the motivations behind the original development of the theory. Nevertheless, the resonant triad model cannot be used to predict the onset of transition in general flows. One obvious problem is that by limiting the analysis to a system of only three interacting modes, resonant triad theory can describe neither a wide-band spectrum of initial disturbances nor the generation of a wide-band spectrum through nonlinear interactions as transition proceeds. Moreover, like linear theory, it predicts an indefinite growth of the disturbances, which ultimately contradicts the starting assumption of weak nonlinearity. Finally, transition may not necessarily occur as a consequence of resonant triad interaction: there exist other, qualitatively different scenarios such as oblique or fundamental breakdowns and wave-vortex interactions, which may initiate transition and which

may require a different type of modeling.

We will therefore discuss other deterministic disturbance evolution models and their implications for statistical modeling.

3.1. Overview of deterministic models. The simplest way to improve the resonant triad model is to increase the number of modes in the analysis. Although this type of model remains restricted to weak nonlinearity, the growing disturbances can be spread over a larger number of modes; the consequent possibility that the amplitude of any one mode can saturate might extend the limits of applicability of the assumption of weak nonlinearity. Evidence supporting this conjecture comes from the analysis of a five-wave resonant system in [53], in which it is found that the effect of additional modes is to delay the onset of explosive nonlinear growth.

Standard perturbation methods can be used to derive governing equations for more complex interactions of wave amplitudes. The simplest generalization of the resonant triad model is [53]

$$(3.1) \qquad \left(\frac{\partial}{\partial t} + W_{1,l} \frac{\partial}{\partial x} + W_{2,l} \frac{\partial}{\partial z} \right) A_l = \gamma_l A_l + \sum_{j,k} h_{l,j+k} S_{ljk} A_j A_k$$

where the indices l, k, j vary over a finite set of modes. In addition to describing the interactions of a larger set of modes, Eq. (3.1) allows for off-resonant interactions through the variation of the phase factor $h_{l,j+k}$. Under strongly off-resonant conditions, the various modes can still communicate through the mean-flow correction (A_0) which is retained in this model. Of course, the significant distortion of mode shapes (and concomitant modification of the growth rates γ_l) under a strong enough mean-flow correction is not explicitly accounted for in the model. The model also allows spanwise modulations of the modal amplitudes.

In the framework of the same perturbation scheme, the equation which incorporates the next order corrections is [53]

$$\left\{ \frac{\partial}{\partial t} + W_{1,l} \frac{\partial}{\partial x} + W_{2,l} \frac{\partial}{\partial z} - \gamma_l - \frac{i}{2} \left(\frac{\partial^2 \omega_l}{\partial \alpha^2} \frac{\partial^2}{\partial x^2} + \frac{\partial^2 \omega_l}{\partial \alpha \partial \beta} \frac{\partial^2}{\partial x \partial z} + \frac{\partial^2 \omega_l}{\partial \beta^2} \frac{\partial^2}{\partial z^2} \right) \right\} A_l$$

$$(3.2) \qquad = \sum_{j,k} \left[\left\{ S_{ljk} A_j A_k + \left(C_{ljk}^{(1)} \frac{\partial A_j}{\partial x} + C_{ljk}^{(2)} \frac{\partial A_j}{\partial z} \right) A_k \right\} h_{i,j+k} + \sum_r C_{ljkr} h_{l,j+k+r} A_j A_k A_r \right].$$

This equation exhibits higher order nonlinearities through the cubic coupling terms, a more complex, amplitude-dependent dispersion through the terms proportional to $C_{ljk}^{(1)}$ and $C_{ljk}^{(2)}$, and dependence on the spatial derivatives of the modal amplitudes. The definitions of all the coefficients are given in the original reference [53].

The question arises whether the higher order models like Eq. (3.2) represent an essential improvement over the lowest order approximation Eq. (3.1). The answer is that this entire class of nonlinear theories has fundamental limitations which are not addressed by formulating higher order theories. As mentioned in the Introduction, this entire class of models can be criticized from the viewpoint of more systematic high Reynolds number asymptotics, because these theories do not properly reduce to linear theory in the far upstream limit. In fact, as noted by [53], the 'self-consistent assignment of harmonics at $x = 0$' constitutes a difficulty for the theory. Moreover, evaluation of the coefficients in terms of linear eigenfunctions shows that their values are dominated by contibutions from nonlinear critical layers. This observation suggests an important role for the nonlinear development of the critical layers.

Both of the above considerations have led to a re-evaluation of triad and generalized triad theories from the standpoint of systematic high Reynolds number asympotic expansions. A representative result is the

integro-differential equation of Goldstein and Lee [14]

$$\frac{dA}{dx} = \frac{4}{5}A + \frac{2}{5}i\int_{-\infty}^{x}(x-x_1)^2 A_3(x_1)A^*(2x-x_1)dx_1$$

$$+i\int_{-\infty}^{x}\int_{-\infty}^{x_1}K_1(x\mid x_1,x_2)A(x_1)A(x_2)A^*(x_1+x_2-2x)dx_2dx_1$$

$$\frac{dA_3}{dx} = (1+i\kappa_i)A_3 - i\int_{-\infty}^{x}\int_{-\infty}^{x_1}[2(x-x_1)^3 A_3(x_1)A(x_2)A^*(2x_1+x_2-2x)+$$

$$K_2(x\mid x_1,x_2)A(x_1)A_3(x_2)A^*(x_1+2x_2-2x)]dx_2dx_1$$

(3.3) $$\qquad +i\int_{-\infty}^{x}\int_{-\infty}^{x_1}\int_{-\infty}^{x_2}K_3(x\mid x_1,x_2,x_3)A(x_1)A(x_2)A_(x_3)A^*(x_1+x_2+x_3-2x)dx_3dx_2dx_1.$$

In this equation, the primary amplitude is A_3, and the subharmonic amplitudes are $A_1 = A_2 = A$. The coefficients κ_i and kernel functions K_i are known in terms of closed-form expressions. All of the relevant definitions are given in [14].

The form of the integral terms on the right sides of Eq. (3.3) show that the solution matches the linear solution in the limit $x \to -\infty$. Achieving the correct matching was indeed the goal of the entire analysis. It is reassuring that, in spite of the differences in the form of the nonlinear term involved, solutions of Eq. (3.3) in fact are qualitatively analogous to those of Craik's model. There is an initial phase of parametric amplification of the subharmonics followed by explosive nonlinear growth of all three modes. The same sensitivity to initial relative phase also exists; the nonlinear growth phase of the evolution can be delayed for certain values of initial phase [14].

A simpler equation than Eq. (3.3) has been derived in [28]:

$$\frac{dA_0}{dx} = \kappa_0 A_0$$

(3.4) $$\frac{dA}{dx} = \kappa_{0b}A + \frac{3\pi}{10}\frac{R^3}{\lambda}iA^*A_0 + iMA(x)\int_0^{\infty}dx'\mid A(x-x')\mid^2$$

The linear growth of the primary suggests purely parametric excitation, but the subharmonic evolution equation contains both an algebraic nonlinearity similar to the Craik model (attributed to a viscous critical layer), and a nonlinear self-interaction term. Indeed, after dropping the self-interaction term, Eq. (3.4) reduces to a special case of Eq. (2.6). Again, all of the notation in Eq. (3.4) is defined in [28]. Analogous theories for other types of wave interactions such as wave-vortex interaction, oblique mode breakdown, and phase-locked interactions have also been developed; see, for instance [10], [50].

While the asymptotic theories have aided greatly in our understanding of the various transition scenarios, each of them pertains to some specific kind of dominant physical balance. Also, in some cases, the underlying asymptotic behavior is only established at impractically large Reynolds numbers. Hence, such models are perhaps not well-suited for engineering prediction of transition. Another transition model, which accounts for mean-flow nonparallelism and disturbance nonlinearity in a composite sense, is the PSE model introduced by Herbert [4], [16]. Albeit not as rigorous as the high Reynolds number asymptotic theories, it is better suited as a general purpose transition prediction tool and has been shown to yield surprisingly accurate predictions through somewhat past the rise of the mean skin-friction curve.

To formulate the PSE for a two-dimensional incompressible mean flow $\mathbf{U}_0(x,y)$, the disturbance field $\hat{\mathbf{u}}(x,y,z,t)$ representing both velocity and pressure is written as a Fourier series

(3.5) $$\hat{\mathbf{u}} = \sum_{m,n}\mathbf{A}_{m,n}(x,y)e^{i(m\beta z - n\omega t)}$$

where the complex amplitudes $\mathbf{A}_{m,n}$ are further decomposed into a slowly varying shape function and a rapidly oscillating phase

(3.6)
$$\mathbf{A}_{m,n}(x,y) = \mathbf{\Psi}_{m,n}(x,y) \exp\left[i \int_{x_0}^{x} \alpha_{m,n}(x')dx'\right].$$

The wavenumbers $\alpha_{m,n}$ are determined so that the downstream evolution of the complex amplitudes $\mathbf{\Psi}_{m,n}$ is as slow and smooth as possible. While there are many alternatives to implement this constraint, a common one is the integral

(3.7)
$$\int dy \ \mathbf{\Psi} \cdot \frac{\partial \mathbf{\Psi}^*}{\partial x} = 0$$

where the asterisk denotes complex conjugation. The above constraint both renders the decomposition in Eq. (3.6) unique and ensures the approximate validity of the marching approximation to the originally elliptic Navier-Stokes equations. The details of this procedure are discussed, for example, in [6].

The final PSE equations can be expressed in the general form

(3.8)
$$\mathsf{D}_{m,n}\mathbf{\Psi}_{m,n} + \mathsf{A}_{m,n}\frac{\partial \mathbf{\Psi}_{m,n}}{\partial x} + \mathsf{B}_{m,n}\frac{\partial \mathbf{\Psi}_{m,n}}{\partial y} = \mathsf{V}_{m,n}\frac{\partial^2 \mathbf{\Psi}_{m,n}}{\partial y^2} + \mathbf{f}_{m,n}.$$

Here the matrices $\mathsf{A}_{m,n}, \cdots \mathsf{D}_{m,n}$ depend on the complex wavenumber $\alpha_{m,n}$ and its streamwise derivatives. The nonlinear forcing term $\mathbf{f}_{m,n}$ can be written as a sum of multilinear forms:

$$\mathbf{f}_{m,n} = \mathbf{f}_{m,n}(\mathbf{\Psi}, \nabla\mathbf{\Psi}) = \sum_{i+k=m, j+l=n} \mathbf{B}_{i,j,k,l}[\mathbf{\Psi}_{i,j}, \nabla\mathbf{\Psi}_{k,l}] \times$$

(3.9)
$$\exp\left[i \int_{x_0}^{x} \alpha_{i,j}(x') + \alpha_{k,l}(x') - \alpha_{m,n}(x')dx'\right].$$

In what follows, the indices on the multilinear forms $\mathbf{B}$ and its arguments will be dropped to simplify the notation.

The mode $\mathbf{\Psi}_{0,0}$ represents the mean flow perturbation. The evolution equation for $\mathbf{\Psi}_{0,0}$

(3.10)
$$\mathsf{D}_{0,0}\mathbf{\Psi}_{0,0} + \mathsf{A}_{0,0}\frac{\partial \mathbf{\Psi}_{0,0}}{\partial x} + \mathsf{B}_{0,0}\frac{\partial \mathbf{\Psi}_{0,0}}{\partial y} = \mathsf{V}_{0,0}\frac{\partial^2 \mathbf{\Psi}_{0,0}}{\partial y^2} + \mathbf{f}_{0,0}$$

contains the mean Reynolds stress gradients $\mathbf{f}_{0,0}$. Hence, the equation for the total mean velocity field $\mathbf{U} = \mathbf{U}_0 + \mathbf{\Psi}_{0,0}$ (where the sum is restricted to velocity components only), is governed by

(3.11)
$$\mathbf{U} \cdot \nabla\mathbf{U} = -\nabla P + \nu\frac{\partial^2 \mathbf{U}}{\partial y^2} + \tilde{\mathbf{f}}_{0,0}$$

where

(3.12)
$$\tilde{\mathbf{f}}_{0,0} = \sum_{m,n \neq 0} \mathbf{B}[\mathbf{\Psi}_{m,n}, \nabla\mathbf{\Psi}_{-m,-n}].$$

The PSE equations provide a closure for the term $\mathbf{f}_{0,0}^*$ since evolution equations for $\mathbf{\Psi}_{m,n}$ are given by Eq. (3.8).

The PSE equation Eq. (3.8) is a type of triple decomposition in which the fluctuations are projected onto components which have known evolution equations rather than being separated into steady and unsteady parts as in Reynolds averaging. The terms $\mathbf{f}_{m,n}$ with $(m,n) \neq (0,0)$ which also arise in the PSE can be understood as generalized Reynolds stress gradients.

17

PSE calculations in this form have typically been carried out only for a short distance past the point at which the skin friction begins to rise. Eventually, the iterative numerical process (which includes nonlinear iterations coupled within the interations required to determine the functions $\alpha_{m,n}$ in Eq. (3.6)) fails to converge before laminar breakdown is completed. To some extent, the nonconvergence may be delayed by treating the nonlinear 'source' term in an implicit fashion ([2]). However, the validity (or at least accuracy) of the PSE model itself becomes questionable in the laminar breakdown region. This region involves a rapid adjustment of the mean flow from laminar to turbulent flow, typically over a rather small number of wavelengths. This means that the terms in $\partial^2/\partial x^2$ are not necessarily negligible, and that the decomposition of the fluctuations into "wave" and "amplitude" components becomes suspect. Only extensive testing will show whether or not the PSE could be applied into the breakdown region. Therefore, from the standpoint of integrated transition and turbulence modeling, it will be desirable to switch over to a conventional turbulence model somewhere in the breakdown region.

3.2. Stochastic formulation: PDF evolution equations for modal amplitudes. We now consider how to recast the deterministic models from Sect. 3.1 in stochastic form, specifically as a closed evolution equation for the joint probability density function of modal amplitudes. These models fall into a natural hierarchy, which progresses from purely algebraic nonlinearity (Eq. (3.1)), to integral nonlinearity (Eq. (3.3)), to a nonlinear partial differential equation (the PSE system Eq. (3.8)). As already noted at the beginning of this section. except for requiring the resolution of a PDF with a very large number of independent modal amplitudes, there is no difficulty in formulating a closed PDF evolution equation corresponding to systems like Eq. (3.1) with purely algebraic nonlinearity. However, the formulation of PDF evolution equations for systems with non-algebraic nonlinearities like Eq. (3.3) and Eq. (3.8) will present closure difficulties.

An expanded set of modes, as suggested in Eq. (3.1), is easily accomodated in the stochastic formulation, at least in principle. The only problem with an expanded set of modes is the practical problem of solving a PDF evolution equation containing a large number of modes. However, deriving evolution equations for the joint probability density function of modal amplitudes corresponding to either high-Reynolds number asymptotic theories or the PSE model introduces a new difficulty because these equations all couple information from different points, either through the spatial derivatives which occur in Eqs. (3.1) and (3.2), or through the spatial integral in Eq. (3.3). This coupling between different points makes it impossible to derive an equation for the single-point probability density without closure assumptions as described below.

In general terms, given an evolution equation for a random field $A(\mathbf{x})$

$$(3.13) \qquad \dot{A} = f(A, \nabla A)$$

where the dot denotes differentiation with respect to the evolution variable, the probability density $\mathcal{P}(A)$ satisfies the continuity equation

$$(3.14) \qquad \frac{\partial \mathcal{P}}{\partial x} = \frac{\partial}{\partial A}\left[\langle f(A, \nabla A) \mid A \rangle \mathcal{P}\right].$$

The unclosed conditional expectation $\langle f(A, \nabla A) \mid A \rangle$ occurs in Eq. (3.14) because the derivative ∇A couples information from any point $\mathbf{x}$ to information from infinitesimally nearby points. The conditional expectation projects this information onto local information at $\mathbf{x}$. As an alternative, it is possible to formulate the continuity equation for $\mathcal{P}$ without conditional expectations, but only as a coupled equation for both $\mathcal{P}$ and the two-point joint probability density $\mathcal{P}^2(A, A')$, where $A = A(\mathbf{x})$ and $A' = A(\mathbf{x}')$. This again leads to an unclosed hierarchy of equations for joint PDF's of higher order.

Conditional expectations do not appear in Craik's triad model, because in the notation of the model Eq. (3.13), f depends only on the local amplitude A, hence trivially

$$(3.15) \qquad \langle f(A) \mid A \rangle = f(A),$$

which allows an immediate closure for the Craik triad system. On the other hand, assuming that the matrix A is invertible, the evolution equation for the probability density $P(\Psi)$ corresponding to the PSE equations Eq. (3.8) is given by

$$\frac{\partial \mathcal{P}}{\partial x} + \frac{\partial}{\partial \Psi} \left\{ \left[\mathsf{A}^{-1} \mathsf{D} \Psi + \mathsf{A}^{-1} \mathsf{B} \left\langle \frac{\partial \Psi}{\partial y} \mid \Psi \right\rangle \right. \right.$$

$$(3.16) \qquad \left. \left. + \mathsf{A}^{-1} \mathsf{V} \left\langle \frac{\partial^2 \Psi}{\partial y^2} \mid \Psi \right\rangle + \mathsf{A}^{-1} \langle \mathbf{f}(\Psi, \nabla \Psi) \mid \Psi \rangle \right] \mathcal{P} \right\} = 0$$

which obviously contains unclosed conditional expectations.

Here we will only outline the simplest, most basic closure scheme for the PDF equation Eq. (3.16), the *conditionally Gaussian* closure [13]. The basis of the closure is the observation that in a Gaussian random field, conditional expectations containing multipoint quantities are all closed by linear regression, which is exact for Gaussian fields. To illustrate this idea, consider the simplest case of a zero mean homogeneous Gaussian random field $\phi(x)$. The Gaussian property implies that the conditional expectation of the field value $\phi(x + r)$ given the value $\phi(x)$ satisfies the linear regression equation

$$(3.17) \qquad \langle \phi(x + r) \mid \phi(x) \rangle = \frac{\langle \phi(x + r) \phi(x) \rangle}{\langle \phi(x)^2 \rangle} \phi(x).$$

Consequently,

$$(3.18) \qquad \langle \phi''(x) \mid \phi(x) \rangle = - \frac{\langle \phi'(x)^2 \rangle}{\langle \phi(x)^2 \rangle} \phi(x)$$

and other derivatives can be evaluated similarly. The conditionally Gaussian closure simply applies results like Eq. (3.18) to a general random field, even if it is non-Gaussian. This step can be compared to the quasi-normal hypothesis often invoked in moment closures.

Of course, application to PSE would involve inhomogeneous random fields. The requisite modifications of Eq. (3.17) are presented in Appendix II. Here, we simply quote the resulting closure for the PSE equation,

$$\frac{\partial \mathcal{P}}{\partial x} + \frac{\partial}{\partial \Psi} \left\{ \left[\mathsf{A}^{-1} \mathsf{D} \Psi + \mathsf{A}^{-1} \mathsf{B} \left(\frac{\partial \langle \Psi \rangle}{\partial y} + \frac{\partial}{\partial y} \mathsf{C}(\Psi, \Psi) \cdot \mathsf{C}(\Psi, \Psi) [\Psi - \langle \Psi \rangle] \right) \right. \right.$$

$$+ \mathsf{A}^{-1} \mathsf{V} \left(\frac{\partial^2 \langle \Psi \rangle}{\partial y^2} + \frac{\partial^2}{\partial y^2} \mathsf{C}(\Psi, \Psi) \cdot \mathsf{C}(\Psi, \Psi) [\Psi - \langle \Psi \rangle] \right)$$

$$+ \mathsf{A}^{-1} \left(\mathbf{f}(\Psi, \frac{\partial}{\partial y} \mathsf{C}(\Psi, \Psi) \cdot \mathsf{C}(\Psi, \Psi) [\Psi - \langle \Psi \rangle], \right.$$

$$(3.19) \qquad \left. \left. \left. \frac{\partial}{\partial x} \mathsf{C}(\Psi, \Psi) \cdot \mathsf{C}(\Psi, \Psi) [\Psi - \langle \Psi \rangle] \Psi \right) \right] \mathcal{P} \right\} = 0$$

This equation contains first and second order statistics of the field Ψ which are defined in terms of the probability density $\mathcal{P}$ by

$$(3.20) \qquad \langle \Psi \rangle = \int d\Psi \ \Psi \mathcal{P}(\Psi)$$

and

(3.21)
$$C(\Psi, \Psi) = \int d\Psi \; \Psi\Psi \mathcal{P}(\Psi)$$

In Eq. (3.21), the product $\Psi\Psi$ is an outer product.

We have not yet addressed the issue of how to implement an integral constraint such as Eq. (3.7) in a stochastic formulation, however, further comments are offered in Sect. 3.3 below. Although Eq. (3.19) provides a complete theory of the evolution of the joint probability density function of modal amplitudes, it must be emphasized that it is based on the assumption of the conditionally Gaussian closure. As in turbulence theory, this assumption cannot be justified *a priori*; its evaluation can only be based on comparisons with experimental or numerical data. Although not be discussed in this work, other closure schemes based on mapping closure or on Wierner-Hermite expansions (Y. Kaneda, private communication) are also possible. However, they will all require a significant effort in terms of formulation, validation, and refinement. Thus, similar to the triad model in Sect. 2, it is worth investigating the application of the particle method to the PSE system.

3.3. Stochastic formulation: truncation of modal amplitude equations and Langevin models for transition.

The particle method will require calculating a large number of individual trajectories with a deterministic model, whether the PSE or other deterministic model. Any PSE calculation obviously will require a truncation of the Fourier series Eq. (3.5) to a finite sum of modes. However, to facilitate the computation of the required number of particle trajectories, it is necessary to further reduce the number of modes retained in whatever deterministic framework is applied for the stochastic analysis. Accordingly, in the present section, we consider how a reduced order model could be obtained as part of the stochastic formulation. This amounts to deriving 'effective' equations governing a limited number of explicitly resolved modes. Such model reduction is particularly important for natural transition, which would contain a wide spectrum of modes at the outset.

For simplicity, consider a general resonant interaction model

(3.22)
$$\dot{A}_i = \gamma_{ij} A_j + C_{ijk} A_j A_k \quad (i, j, k = 1, N)$$

where the matrix γ_{ij} is diagonal, so that there is no linear coupling between the modes.

Suppose that the modes can be divided into two sets: slow, large amplitude resolved modes A^+, the modes A_i with $1 \leq i \leq N_r$, and fast, small amplitude unresolved modes A^-, the modes A_i with $N_r < i \leq N$. Let it be required to model the evolution of the complete system by solving modified equations for the resolved modes alone. It is possible to rewrite Eq. (3.22) for the resolved modes in the form

(3.23)
$$\begin{aligned} \dot{A}_i^+ &= \left(\gamma_{ip} + C_{ipr} A_r^- \right) A_p^+ + C_{ipq} A_p^+ A_q^+ + C_{irs} A_r^- A_s^- \\ &= \gamma_{ip}^* A_p^+ + C_{ipq} A_p^+ A_q^+ + f_i \end{aligned}$$

where we have introduced the effectively modified linear growth rates

(3.24)
$$\gamma_{ip}^* = \gamma_{ip} + g_{ip}$$

where

(3.25)
$$g_{ip} = C_{ipr} A_r^-$$

and the forcing attributed to unresolved interactions

$$(3.26) \qquad\qquad f_i = C_{irs}A_r^- A_s^-.$$

At this point, Eq. (3.23) is nothing more than a formal restatement of the original equations Eq. (3.22). But since the unresolved modes are assumed to vary rapidly compared to the resolved modes, it may be reasonable to replace the terms f_i and g_{ip} in Eq. (3.26) by random quantities with statistics to be evaluated from the resolved part of the motion. Thus, we replace the term f_i by a random force with correlation function

$$(3.27) \qquad\qquad \langle f_i f_j \rangle = C_{irs}C_{jlm}\langle A_r^- A_s^- A_l^- A_m^- \rangle.$$

and the quantity g_{ip} by a random tensor with correlation function

$$(3.28) \qquad\qquad \langle g_{ip}g_{jq} \rangle = C_{ipr}C_{jqs}\langle A_r^- A_s^- \rangle$$

This approximation replaces the problem of explicitly computing the evolution of the unresolved modes with the problem of modeling of the correlations on the right sides of Eqs. (3.27) and (3.28).

Eq. (3.23) shows that the unresolved modes modify the linear growth rates and act as a random force on the resolved modes. These effects will reduce the phase coherence of the resolved modes and could consequently prevent the indefinite growth of the disturbance amplitudes. One may also observe this on the basis of the PDF evolution equation for this model. In the absence of any random forcing, the PDF evolution equation only contains spatial derivatives of the convective type (see Eq. (2.12)). Random forcing will add diffusive terms to this equation and diffusion will counteract the tendency toward phase coherence exhibited, for example, in Fig. (2.4). The link between the reduction of phase coherence and the suppresion of modal amplitude growth is demonstrated experimentally in Refs. [9] and [29]. Another viewpoint on this link in the context of resonant triad theory appears in Ref. [48], which observes that higher-order nonlinearity of the type exhibited in Eq. (3.2) causes amplitude-dependent reduction of phase coherence, which entirely suppresses explosive growth.

To investigate the connection between reduced phase coherence and inhibition of subharmonic growth more closely, we repeated the simpler triad computation from Ref. [53] after modifying the phase in Eq. (2.23) by adding white noise of various amplitudes to its right hand side. This phase randomization is equivalent to randomization of the coefficient matrices in the modified PSE equations Eq. (3.45). Specifically, we set

$$(3.29) \qquad \dot{\theta} = \frac{r_1 r_2}{r_3}\sin(\phi - \theta) - \frac{r_1 r_3}{r_2}\sin\theta - \frac{r_2 r_3}{r_1}\sin\theta + Aw(x)$$

where $w(x)$ is a white noise process and the amplitude A was set equal to 0.010, 0.050, 0.100, 0.200. The degree of phase decorrelation caused by the random forcing is revealed by comparing the phase evolution shown in the left-hand plots in Figs. 3.1–3.4 with the phase evolution in the absence of random forcing shown in Fig. 2.6. At the smallest noise amplitude $A = 0.010$, the phase locking near $\theta = 0$ is only weakly perturbed: the phase fluctuates by about 0.1π about the deterministic value. At this level of phase randomization, the nonlinear evolution of the phase dominates the effect of random forcing. But when $A = 0.200$, it is apparent that the phase evolution is almost entirely dominated by the random forcing, and the phase appears to evolve as a Brownian motion. Correspondingly, subharmonic growth is almost entirely suppressed in this case. Intermediate values of the noise amplitude delay the crossover between the amplitudes of the subharmonics and the primary.

We stress that in Figs. 3.1–3.4, the suppression of energy growth in the subharmonics has been accomplished entirely through phase randomization: energy has not been removed from the system directly in these calculations. In effect, the phase-locked attractor, which promotes subharmonic growth, has been destroyed by stochasticity.

Another viewpoint on the connection between phase coherence and nonlinear growth is through the *bicoherence* [29], [35]. This statistic is a third-order joint moment which measures the correlation between one modal amplitude and the product of two others. Large bicoherence indicates strong triadic coupling between modes, which cannot be revealed by second-order statistics. Experimentally, it has been observed that in forced transition, the bicoherence spectrum is initially strongly peaked, indicating three-mode resonance. As transition proceeds, the bicoherence spectrum broadens and weakens, indicating that more modes are coupled to each other, but that the degree of correlation between them has been reduced. In future work, we will consider the possibility of modeling this aspect of transition through stochastic PSE models, which have a more general validity than the present stochastic triad model.
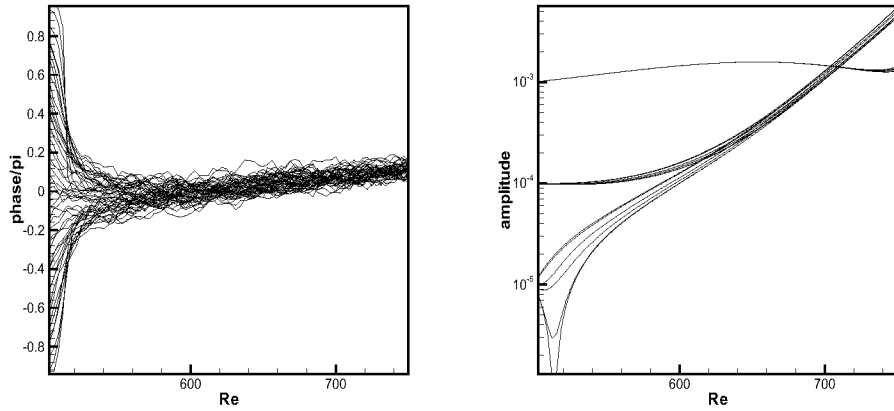

FIG. 3.1. *Effect of random noise perturbation of phase evolution equation on subharmonic amplification during resonant triad evolution. The conditions are those of Fig. 2.6, with white-noise perturbation of the phase evolution equation Eq. (3.29 with amplitude $A = 0.010$.*

To complete the reduced-order modeling, the correlations Eqs. (3.27) and (3.28) must be expressed in terms of the resolved fields alone. As an example of a possible approximation, suppose that the amplitudes of the unresolved modes are small enough that nonlinear interactions among them can be ignored. This approximation leads to the simple "driven-mode" approximation

$$(3.30) \qquad \dot{A}_i^- = \gamma_{ij} A_j^- + C_{ijk} A_j^+ A_k^+.$$

This equation can be solved explicitly in the form

$$(3.31) \qquad A_i^-(x) = \int_0^x dy \, G_{ii'}(x-y) C_{i'jk}(y) A_j^+(y) A_k^+(y)$$

where

$$(3.32) \qquad G_{ii'}(x-y) \delta_{ii'} e^{-\gamma_{ii}(x-y)}$$

is the linear response. The substitution of Eq. (3.31) for the amplitudes A_i^- in Eqs. (3.27) and (3.28) achieves the goal of expressing these correlations in terms of the resolved modes A_i^+.

FIG. 3.2. *Effect of random noise perturbation of phase evolution equation on subharmonic amplification during resonant triad evolution. The conditions are those of Fig. 2.6, with white-noise perturbation of the phase evolution equation Eq. (3.29 with amplitude $A = 0.050$.*

FIG. 3.3. *Effect of random noise perturbation of phase evolution equation on subharmonic amplification during resonant triad evolution. The conditions are those of Fig. 2.6, with white-noise perturbation of the phase evolution equation Eq. (3.29 with amplitude $A = 0.100$.*

Because it uses the linear response function Eq. (3.32) to eliminate the unresolved modes, this approximation can be compared to the quasi-normal theory of turbulence. A refinement is offered by the direct interaction approximation (DIA) [23]. This approximation was developed as a statistical closure theory for systems with a large number of nonlinearly coupled modes. Applied to a general system with a quadratic nonlinearity, the basic assumption behind this approximation is that the nonlinear interactions among any specific modal triad may be treated as small, although the overall effect of all possible triad interactions may nevertheless be quite significant.

The DIA improves on the quasi-normal theory by replacing the linear response function of Eq. (3.32) by a generalized response function defined as follows. First, evaluate the linearized equation for the response of
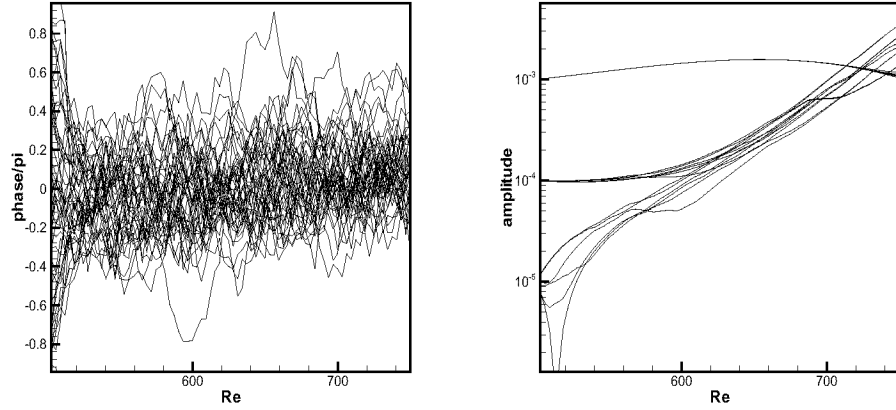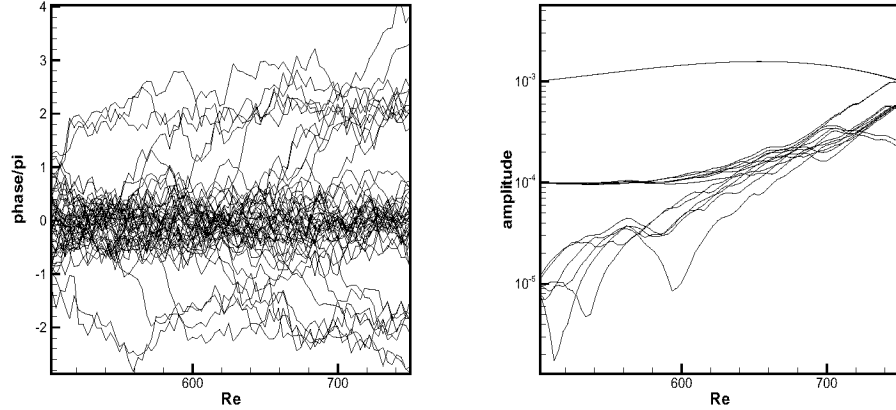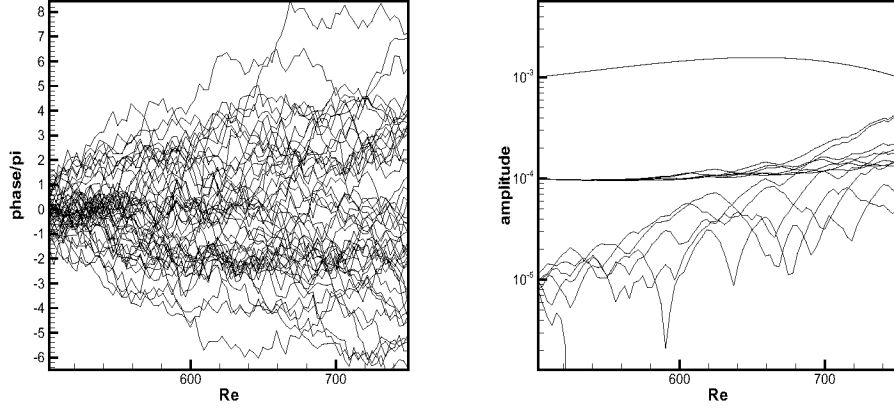
FIG. 3.4. *Effect of random noise perturbation of phase evolution equation on subharmonic amplification during resonant triad evolution. The conditions are those of Fig. 2.6, with white-noise perturbation of the phase evolution equation Eq. (3.29 with amplitude $A = 0.200$.*

A^- to an infinitesimal perturbation ξ_i as

$$(3.33) \qquad \delta \dot{A}_i^- = \gamma_{ij} \delta \dot{A}_j^- + C_{ijk} \delta \dot{A}_j^- A_k^- + C_{ijk} A_j^- \delta \dot{A}_k^- + \xi_i.$$

The generalized response function is defined as the average 'sensitivity matrix'

$$(3.34) \qquad G_{ij} = \left\langle \frac{\delta \dot{A}_i^-}{\delta \xi_j} \right\rangle$$

which replaces the linear response function Eq. (3.32) in Eq. (3.28). The theory is completed by an evolution equation for the response matrix G_{ij}. In the context of transition theory, the generalized response function can perhaps be compared to the quantities α of the PSE: unlike linear theories based on the Orr-Sommerfeld equation, PSE determines these functions in a fully nonlinear, coupled fashion. Similarly, the DIA response function replaces the linear response by a quantity which accounts for nonlinear interactions.

Note that the integration in Eq. (3.32) introduces history effects, similar to the high-Reynolds number asymptotic models. This again introduces closure difficulties for stochastic formulations of the amplitude evolution equations.

3.4. Link to turbulence modeling. The results of Sects. 3.2 and 3.3 will now be applied to the PSE equations. Our goal is to develop a usable stochastic form of the PSE equations in which only a reasonably small set of modes is resolved explicitly, and the effects of the remaining modes is modeled through random forces and random coefficients. This model will provide a natural interface between transition modeling and turbulence modeling if the unresolved motion can be characterized statistically by a turbulence model.

The breakdown of PSE calculations shortly after the rise in the skin friction coefficient has been discussed in Sect. 3.2.1. To continue the PSE past this point, and perhaps even into the fully turbulent region, we will assume that the PSE model would be adequate if the basis of modes could be expanded indefinitely; but rather than explicitly resolving the new modes generated during the phase of rapid spectral broadening by PSE, we will treat them as unresolved components of the motion to be modeled following Eq. (3.23). Since these modes are both faster in time scale and smaller in amplitude than the resolved modes, this type

of modeling is reasonable. Our contention will be that a randomized PSE model will provide two required parts of an integrated turbulence and transition model, namely a transition-like model which applies into the breakdown region, and which interfaces naturally with a RANS model which will be applied in the fully turbulent region.

Following the notation of Sect. 3.3, we decompose the disturbance into resolved and unresolved modes as

$$
\hat{\mathbf{u}} = \sum_{|m|\leq M,|n|\leq N} \mathbf{A}^+_{m,n}(x,y)e^{i(m\beta z - n\omega t)} + \sum_{|m|>M,|n|\leq N} \mathbf{A}^-_{m,n}(x,y)e^{i(m\beta z - n\omega t)}
$$

(3.35)
$$
+ \sum_{|m|\leq M,|n|>N} \mathbf{A}^-_{m,n}(x,y)e^{i(m\beta z - n\omega t)} + \sum_{|m|>M,|n|>N} \mathbf{A}^-_{m,n}(x,y)e^{i(m\beta z - n\omega t)}
$$

where the $+$ modes will be resolved explicitly and the $-$ modes will be modeled. After applying the wave-amplitude decomposition Eq. (3.5), the resolved modes are found to satisfy the equations

(3.36) $\mathsf{D}_{m,n}\boldsymbol{\Psi}^+_{m,n} + \mathsf{A}_{m,n}\dfrac{\partial \boldsymbol{\Psi}^+_{m,n}}{\partial x} + \mathsf{B}_{m,n}\dfrac{\partial \boldsymbol{\Psi}^+_{m,n}}{\partial y} = \mathsf{V}_{m,n}\dfrac{\partial^2 \boldsymbol{\Psi}^+_{m,n}}{\partial y^2} + \mathbf{f}_{m,n}(\boldsymbol{\Psi}^+,\nabla\boldsymbol{\Psi}^+) + \mathbf{F}_{m,n}(\boldsymbol{\Psi}^-,\nabla\boldsymbol{\Psi}^-)$

where the contributions from the unresolved modes appear in the term $\mathbf{F}_{m,n}$ which is defined by

(3.37) $\qquad \mathbf{F}_{m,n}(\boldsymbol{\Psi}^-,\nabla\boldsymbol{\Psi}^-) = \mathbf{f}_{m,n}(\boldsymbol{\Psi}^-,\nabla\boldsymbol{\Psi}^+) + \mathbf{f}_{m,n}(\boldsymbol{\Psi}^+,\nabla\boldsymbol{\Psi}^-) + \mathbf{f}_{m,n}(\boldsymbol{\Psi}^-,\nabla\boldsymbol{\Psi}^-)$

and the terms on the right side of Eq. (3.37) are defined by

(3.38) $\qquad \mathbf{f}_{m,n}(\boldsymbol{\Psi}^-,\nabla\boldsymbol{\Psi}^+) = \displaystyle\sum_{i+i'=m,j+j'=n} \mathbf{B}[\boldsymbol{\Psi}^-_{i,j},\nabla\boldsymbol{\Psi}^+_{i',j'}]\Delta_{i,j,i',j',m,n}$

(3.39) $\qquad \mathbf{f}_{m,n}(\boldsymbol{\Psi}^+,\nabla\boldsymbol{\Psi}^-) = \displaystyle\sum_{i+i'=m,j+j'=n} \mathbf{B}[\boldsymbol{\Psi}^+_{i,j},\nabla\boldsymbol{\Psi}^-_{i',j'}]\Delta_{i,j,i',j',m,n}$

(3.40) $\qquad \mathbf{f}_{m,n}(\boldsymbol{\Psi}^-,\nabla\boldsymbol{\Psi}^-) = \displaystyle\sum_{i+i'=m,j+j'=n} \mathbf{B}[\boldsymbol{\Psi}^-_{i,j},\nabla\boldsymbol{\Psi}^-_{i',j'}]\Delta_{i,j,i',j',m,n}$

where

(3.41) $\qquad \Delta_{i,j,i',j',m,n} = \exp\left[i\displaystyle\int_{x_0}^x \alpha_{i,j}(x') + \alpha_{i',j'}(x') - \alpha_{m,n}(x')dx'\right]$

For brevity of notation, restrictions on the summation ranges in Eq. (3.40) which arise from the definitions in Eq. (3.35) have been omitted in Eqs. (3.38)–(3.40).

The modified PSE Eq. (3.37) can be rewritten as

$$
\sum_{m',n'}\left[\mathsf{D}'_{m,n,m',n'}\boldsymbol{\Psi}^+_{m',n'} + \mathsf{A}'_{m,n,m',n'}\dfrac{\partial \boldsymbol{\Psi}^+_{m',n'}}{\partial x} + \mathsf{B}'_{m,n,m',n'}\dfrac{\partial \boldsymbol{\Psi}^+_{m',n'}}{\partial y}\right]
$$

(3.42)
$$
= \mathsf{V}_{m,n}\dfrac{\partial^2 \boldsymbol{\Psi}^+_{m,n}}{\partial y^2} + \mathbf{f}_{m,n}(\boldsymbol{\Psi}^+,\nabla\boldsymbol{\Psi}^+) + \mathbf{q}_{m,n}
$$

where the new convective coefficients include the effects of unresolved modes:

(3.43) $\qquad \displaystyle\sum_{m',n'} \mathsf{D}'_{m,n,m',n'}\boldsymbol{\Psi}^+_{m',n'} = \mathsf{D}_{m,n}\boldsymbol{\Psi}^+_{m,n} + \mathbf{f}_{m,n}(\boldsymbol{\Psi}^+,\nabla\boldsymbol{\Psi}^-)$

(3.44) $\qquad \displaystyle\sum_{m',n'} \mathsf{A}'_{m,n,m',n'}\dfrac{\partial \boldsymbol{\Psi}^+_{m',n'}}{\partial x} = \mathsf{A}_{m,n}\dfrac{\partial \boldsymbol{\Psi}^+_{m,n}}{\partial x} + \mathbf{f}_{m,n}(\boldsymbol{\Psi}^-,\dfrac{\partial\boldsymbol{\Psi}^+}{\partial x})$

(3.45) $\qquad \displaystyle\sum_{m',n'} \mathsf{B}'_{m,n,m',n'}\dfrac{\partial \boldsymbol{\Psi}^+_{m',n'}}{\partial y} = \mathsf{B}_{m,n}\dfrac{\partial \boldsymbol{\Psi}^+_{m,n}}{\partial y} + \mathbf{f}_{m,n}(\boldsymbol{\Psi}^-,\dfrac{\partial\boldsymbol{\Psi}^+}{\partial y})$

and the forcing term

$$(3.46) \qquad \mathbf{q}_{m,n} = \mathbf{f}_{m,n}(\boldsymbol{\Psi}^-, \nabla \boldsymbol{\Psi}^-)$$

contains contributions from unresolved modes alone.

Eqs. (3.42)–(3.46) simply restate the PSE equations with a larger set of modes. The goal now is to model the effect of the added fields $\boldsymbol{\Psi}^-$ without explicitly resolving them, as in large eddy simulations of turbulence. One approach would be to develop approximate equations of evolution for the unresolved scales in terms of the resolved scales. Instead, it is also possible to treat the random couplings in Eqs. (3.43)–(3.45) and the term $\mathbf{q}_{m,n}$ in Eq. (3.46) as Gaussian random processes with statistics determined by the resolved fields as discussed in Sect. 3.2. When this is done, the original PSE is replaced by a Langevin-like model which includes a random force. Unlike a strict Langevin model, in which a random force is added to a deterministic equation, the model proposed here will have both a random force and random coefficients. Applications of Langevin models to turbulence theory have been proposed by [31].

The random force $\mathbf{q}_{m,n}$ has the correlation function

$$(3.47) \qquad \left\langle \mathbf{q}_{m,n}\, \mathbf{q}_{-m,-n} \right\rangle = \sum_{i+i'=m,\ j+j'=n,\ k+k'=-m,\ l+l'=-n} \left\langle \mathbf{B}[\boldsymbol{\Psi}^-_{k,l}, \nabla \boldsymbol{\Psi}^-_{k',l'}] \right\rangle$$

Note, first, that Eq. (3.47) defines a space-time correlation and, second, the process $\mathbf{q}$ is not white noise in time.

We will outline one particular model, suggested by Sect. 3.2, to close the PSE equations for resolved modes. To begin, replace the complete PSE equation for the unresolved modes, following Eq. (3.23) by

$$(3.48) \qquad \mathsf{D}_{m,n}\boldsymbol{\Psi}^-_{m,n} + \mathsf{A}_{m,n}\frac{\partial \boldsymbol{\Psi}^-_{m,n}}{\partial x} + \mathsf{B}_{m,n}\frac{\partial \boldsymbol{\Psi}^-_{m,n}}{\partial y} = \sum_{i+i'=m, j+j'=n} \mathbf{B}[\boldsymbol{\Psi}^+_{i,j}, \nabla \boldsymbol{\Psi}^+_{i',j'}].$$

In making this approximation, we argue that the disturbances represented by the mode amplitudes $\boldsymbol{\Psi}^-$ are small compared to the resolved disturbances $\boldsymbol{\Psi}$. Then it is reasonable to ignore the nonlinearity of the $\boldsymbol{\Psi}^-$ evolution equations and treat the $\boldsymbol{\Psi}^-$ modes as driven by the resolved modes.

The matrices $\mathsf{A} \cdots \mathsf{D}$ in Eq. (3.48) contain the complex growth rates $\alpha_{m,n}$ which are found in PSE as part of the modal evolution. Since the $\boldsymbol{\Psi}^-$ modes are not to be explicitly resolved, one might replace these quantities by the linear growth rates obtained by linearizing the governing equations about the resolved disturbance

$$(3.49) \qquad \hat{\mathbf{u}}^0 = \sum_{|m|\leq M, |n|\leq N} \mathbf{A}_{m,n}(x,y)e^{i(m\beta z - n\omega t)}.$$

With this prescription for the complex growth rates, Eq. (3.48) is determinate, and the force correlation Eq. (3.47) can be evaluated in terms of the resolved disturbance alone.

By specializing to the $(m,n) = (0,0)$ mode, we can form the equation for the mean flow modification. In this equation, the amplitude of the random perturbation $\boldsymbol{\Psi}^-_{0,0}$ can be expected to grow in comparison to the resolved stresses $\mathbf{q}_{0,0}$. As noted earlier, the sum $\boldsymbol{\Psi}^-_{0,0} + \mathbf{q}_{0,0}$ defines the Reynolds stress gradients. Although the PSE Langevin model is a completely consistent turbulence theory, in the interests of economical calculations, it can be replaced by a turbulence model once the random contribution dominates the contribution from the resolved modes. Relevant switchover strategies of this type have been proposed in a somewhat different context by Spalart [42] for detached eddy simulation and by Speziale [43] for combining DNS with RANS.

It is also of some interest to note that the PSE equations include a kind of two-equation model. To derive this model, we replace the modal amplitude vector $\mathbf{\Psi}$ by a vector $\tilde{\mathbf{\Psi}}$ in which the amplitude components pertain only to the velocities. Indeed, multiplying Eq. (3.8) by $\tilde{\mathbf{\Psi}}^*_{m,n}$ gives a disturbance energy equation,

$$(3.50) \quad \tilde{\mathbf{\Psi}}^*_{m,n}\mathsf{D}_{m,n}\tilde{\mathbf{\Psi}}_{m,n} + \tilde{\mathbf{\Psi}}^*_{m,n}\mathsf{A}_{m,n}\frac{\partial \tilde{\mathbf{\Psi}}_{m,n}}{\partial x} + \tilde{\mathbf{\Psi}}^*_{m,n}\mathsf{B}_{m,n}\frac{\partial \tilde{\mathbf{\Psi}}_{m,n}}{\partial y} = \tilde{\mathbf{\Psi}}^*_{m,n}\mathsf{V}_{m,n}\frac{\partial^2 \tilde{\mathbf{\Psi}}_{m,n}}{\partial y^2} + \tilde{\mathbf{\Psi}}^*_{m,n}\mathbf{f}_{m,n}.$$

Since $\mathbf{\Psi}$ is a vector and the quantities $\mathsf{A}\cdots\mathsf{D}$ are matrices, the products in Eq. (3.50) are all scalars. The effective dissipation rate in this equation is the last term, $\tilde{\mathbf{\Psi}}^*_{m,n}\mathbf{f}_{m,n}$; its equation, also found from Eq. (3.8) is

$$(3.51) \quad \mathbf{f}_{m,n}\mathsf{D}_{m,n}\tilde{\mathbf{\Psi}}^*_{m,n} + \mathbf{f}_{m,n}\mathsf{A}_{m,n}\frac{\partial \tilde{\mathbf{\Psi}}^*_{m,n}}{\partial x} + \mathbf{f}_{m,n}\mathsf{B}_{m,n}\frac{\partial \tilde{\mathbf{\Psi}}^*_{m,n}}{\partial y} = \mathbf{f}_{m,n}\mathsf{V}_{m,n}\frac{\partial^2 \tilde{\mathbf{\Psi}}^*_{m,n}}{\partial y^2} + \mathbf{f}_{m,n}\mathbf{f}^*_{m,n}.$$

Note that the above dissipation rate represents only the nonlinear energy transfer from large to small scales. It ignores viscous dissipation; in that sense, it may differ from the total dissipation rate used in conventional two-equation models.

We conclude by briefly discussing how the PDF equation for PSE modal amplitudes can be modified to account for the random force introduced above as a model for the unresolved modes. A complete PDF model for the stochastic PSE cannot be formulated exactly, because of the implicit procedure used to determine the growth rates α. The evolution of these quantities is highly path dependent, and it is impossible to construct a stochastic model of the evolution of all possible transition paths. Also, the appearance of stochastic coefficients will require extensions to the standard methods. Thus, the present discussion will be limited to a very special case, namely we will assume that the α can be determined once and for all for all paths, and only the effect of the random force term $\mathbf{q}$ will be considered.

Using the conditionally Gaussian closure, the modified equations will have the form

$$
\begin{aligned}
&\frac{\partial \mathcal{P}}{\partial x} + \frac{\partial}{\partial \mathbf{\Psi}}\left\{\left[\mathsf{A}^{-1}\mathsf{D}\mathbf{\Psi} + \mathsf{A}^{-1}\mathsf{B}\left(\frac{\partial \langle \mathbf{\Psi}\rangle}{\partial y}\right.\right.\right.\\
&\left.+\frac{\partial}{\partial y}\mathsf{C}(\mathbf{\Psi},\mathbf{\Psi})\cdot\mathsf{C}(\mathbf{\Psi},\mathbf{\Psi})[\mathbf{\Psi}-\langle\mathbf{\Psi}\rangle]\right)\\
&+\mathsf{A}^{-1}\mathsf{V}\left(\frac{\partial^2 \langle\mathbf{\Psi}\rangle}{\partial y^2} + \frac{\partial^2}{\partial y^2}\mathsf{C}(\mathbf{\Psi},\mathbf{\Psi})\cdot\mathsf{C}(\mathbf{\Psi},\mathbf{\Psi})[\mathbf{\Psi}-\langle\mathbf{\Psi}\rangle]\right)\\
&+\mathsf{A}^{-1}\left(\mathbf{f}(\mathbf{\Psi},\frac{\partial}{\partial y}\mathsf{C}(\mathbf{\Psi},\mathbf{\Psi})\cdot\mathsf{C}(\mathbf{\Psi},\mathbf{\Psi})[\mathbf{\Psi}-\langle\mathbf{\Psi}\rangle],\right.\\
&\left.\left.\left.\frac{\partial}{\partial x}\mathsf{C}(\mathbf{\Psi},\mathbf{\Psi})\cdot\mathsf{C}(\mathbf{\Psi},\mathbf{\Psi})[\mathbf{\Psi}-\langle\mathbf{\Psi}\rangle]\mathbf{\Psi}\right)\right]\mathcal{P}\right\}\\
&+\mathsf{A}^{-1}\left\{\frac{\partial^2 \mathcal{P}}{\partial\mathbf{\Psi}\partial\mathbf{\Psi}}\langle\mathbf{\Psi}\mathbf{\Psi}\rangle + \frac{\partial^2 \mathcal{P}}{\partial\mathbf{\Psi}\partial\mathbf{\Psi}_{,x}}\left\langle\mathbf{\Psi}\frac{\partial\mathbf{\Psi}}{\partial x}\right\rangle\right.\\
&\left.+\frac{\partial^2 \mathcal{P}}{\partial\mathbf{\Psi}\partial\mathbf{\Psi}_{,y}}\left\langle\mathbf{\Psi}\frac{\partial\mathbf{\Psi}}{\partial y}\right\rangle + \frac{\partial^2 \mathcal{P}}{\partial\mathbf{\Psi}_{,x}\partial\mathbf{\Psi}_{,y}}\left\langle\frac{\partial\mathbf{\Psi}}{\partial x}\frac{\partial\mathbf{\Psi}}{\partial y}\right\rangle\right\} = 0.
\end{aligned}
$$

(3.52)

Again, the crucial effect of the random force appears in the last two lines of Eq. (3.52) which are diffusive terms indicative of the weakening of modal correlations. These diffusive terms again have the effect of preventing the indefinite buildup of modal phase correlations, a critical feature of any theory which proposes to integrate the dynamics of transition and of turbulence. We stress, however, that numerical solution of Eq. (3.52) is probably impractical.

Could a model like Eq. (3.52) be used in practice? The large number of degrees of freedom could perhaps be handled by the particle method, by finding a simpler system than the stochastic PSE equations for which

the PDF of the modal amplitudes is also governed by Eq. (3.52). This recommendation of Pope [31] has been succesfully applied to problems like reacting flows, which in a Lagrangian frame reduce to ordinary differential equations. In the present problem, the 'paths' are evolving fields described by partial differential equations. Extension of the particle method to this class of problems will require further generalization of the basic particle method formulation. The more fundamental problem for stochastic formulation of the PSE is that each transition path will correspond to a distinct evolution of the complex wavenumbers $\alpha_{m,n}$. Thus, even more approximations will be needed to formulate the PSE in a fully stochastic setting.

4. Summary and future work. Integrated modeling of transition and turbulence has emerged as a crucial need in many practical aerodynamic applications. To retain the physical basis necessary to explain the relevant parametric dependencies and, hence, achieve the desired prediction accuracy, such integrated computations must be done seamlessly over the entire transition process, from the initial disturbances to fully developed turbulence. Thus, two levels of integration are inherent to an approach of this type, a coupled prediction of the laminar-through-transitional and turbulent regions of the flowfield (at the top) and an integrated prediction of the various stages of transition (on the tier underneath). In addition, it is desirable to pose the transition prediction problem in a stochastic context, in order to both facilitate an easy interface with the statistical models for turbulence and to quantify the effect of randomness and/or uncertainties associated with the input quantities that are required for transition prediction. The present work may be regarded as an embryonic attempt to explore the above needs, with an emphasis on the stochastic aspects of nonlinear disturbance evolution in a laminar boundary layer and its potential continuation into the regions of laminar breakdown as well as the fully turbulent flow downstream.

The fundamental properties of resonant wave interactions in boundary layer flows are that subharmonics can grow rapidly through parametric excitation, and that parametric growth is typically followed by an explosive nonlinear growth of all modal amplitudes. The explosive growth phase can be delayed if the initial phases are suitably related. Our calculations confirm these findings by previous researchers and quantify the dependence of disturbance amplitudes on the initial conditions by evaluating the evolution of their joint probability density function for a given description of the initial disturbances not in deterministic terms, but in terms of corresponding statistical measures.

A basic objection to both linear stability theory and resonant interaction theory is that the predicted indefinite amplification of disturbances is not observed, even though the mean flow could in principle provide an energy source for such growth. 'Nonlinearity,' without further qualification, is sometimes cited as the reason for the saturation of the disturbance amplitude; but even the spreading of the disturbance over every more modes is not an explanation. Instead, the prevention of the development of strong phase correlations by coupling to a larger set of modes appears to have a significant role as well. Therefore, in developing an integrated theory of transition and turbulence, it will be important to recognize the proper role of phase correlations in determining the onset of transition.

The probabilistic analysis has been extended to the PSE equations, which are to date the most comprehensive, albeit non-rigorous, model for engineering prediction of laminar-turbulent transition. The crossover from the PSE equations to a turbulence model has been described through a PSE Langevin model, in which the PSE equations are modified by random forces and random dephasing terms. When the random perturbations grow sufficiently, the PSE Langevin model can be replaced by a RANS model in the interest of economy of computation.

Our conclusion is that a stochastic formulation of the PSE transition model can link transition modeling and turbulence modeling in the required seamless fashion. Stochastic closures for unresolved motions are the

most important requirement. The recommendations in Sect. 3.3 were based directly on transition theory, but an interesting alternative (which may be easily implemented in practice) would be to apply the ideas of large eddy simulation to formulate analogs of the Smagorinsky and dynamic Smagorinsky model appropriate to transitional flows within the PSE framework. This approach has the potential to make the crossover to turbulence models much more straightforward.

The primary motivation behind considering reduced-order models for PSE was to facilitate engineering predictions through the transition region. However, another benefit would be to provide detailed physical insights into the transition process via a coupled PSE-LES/DNS approach. Essentially by extending the PSE predictions further into the laminar breakdown region, the computational domain for LES/DNS could significantly shortened (see, for example, [19], [32]). Indeed, if PSE calculations can be successfully continued even into the turbulent region, there is the interesting possibility of being able to predict sublayer dynamics including wall streaks and bursting frequencies. Application of PSE in this respect offers an attractive alternative to other modal analyses of fully turbulent flows which have been pursued over many years ([54], [47]). Of course, to make this application feasible, extensive comparisons against numerical and, where available, experimental databases will have to be carried out. We also plan to conduct an *a priori* analysis of the simulation data, both in order to evaluate the accuracy of candidate models for residual stress components and to ascertain the validity of PSE methodology past the onset of transition.

So far, we have focused our attention on stochastic, integrated prediction of the transition process. The next phase of this work will involve linking transition prediction and conventional CFD codes. In brief, the overall computation involves an iterative procedure consisting of a RANS computation over the entire flow field coupled with an 'unsteady' computation (PSE and residual stress) over the laminar and transitional region. The mean flow (obtained directely from RANS or via a boundary layer solver) is fed from the RANS model to the transitional module, which predicts the extent of the laminar and transitional regions, plus the mean Reynolds stress distribution. This information, in turn, is injected into the RANS simulation. This procedure is analogous to 'zonal' modeling for fully turbulent flow fields, except that the zonal boundaries are not predetermined in our case (also, the unsteady calcualtion may take place over a different grid using spatial marching approach instead of a pseudo-time marching typical of RANS calculations). A robust implementation of this procedure will require special attention to numerical convergence of the global iteration procedure. Other related numerical issues have recently been investigated in [44].

<div align="center">REFERENCES</div>

[1] R. ABID, *Evaluation of two-equation turbulence models for predicting transitional flows*, Int. J. Eng. Sci. **31** (1993), pp. 831-840.

[2] P. BALAKUMAR, *Transition and breakdown to turbulence in incompressible boundary layer*, Final report on NASA Grant NAG1-1934, Nov. 1998.

[3] F. P. BERTOLOTTI AND J. D. CROUCH, *Simulation of boundary-layer transition: Receptivity to spike stage*, ICASE Report 92-72, 1992.

[4] F. BERTOLOTTI, T. HERBERT, AND P. R. SPALART, *Linear and nonlinear stability of the Blasius boundary layer*, J. Fluid Mech. **242** (1992), pp. 441-474.

[5] D. M. Bushnell and M. R. Malik, *Application of stability theory to laminar flow control – progress and requirements*, Proceedings of Symposium on Time Dependent and Spatially Varying Flows, NASA Langley Research Center, edited by D. L. Dwoyer and M. Y. Hussaini (Springer-Verlag, New York), pp. 1-17 (1987).

[6] C.-L. Chang and M. R. Malik, *Oblique-mode breakdown in supersonic boundary layers*, J. Fluid Mech. **273** (1994), pp. 323-360.

[7] C. L. Chang, B. A. Singer, S. P. G. Dinavahi, N. M. El-Hady, C. D. Pruett, J. E. Harris, C. L. Streett, T. A. Zang, D. C. Wilcox, *Transition region modeling for compressible flow*, AIAA Paper 92-5066 (1992).

[8] M. Choudhari, *Boundary layer receptivity due to distributed surface imperfections of a deterministic or random nature*, Theor. Comput. Fluid Dyn. **4** (1993), pp. 101-118.

[9] T. C. Corke and R. A. Mangano, *Resonant growth of three-dimensional modes in transitioning Blasius boundary layers*, J. Fluid Mech. **209** (1989), pp. 93-150.

[10] S. C. Cowley and X. Wu, *Asymptotic approaches to Transition modeling*, AGARD R-793 (1994), pp. 3.1-3.38.

[11] T.J. Craft, B.E. Launder, and K. Suga, *Prediction of turbulent transitional phenomena with a nonlinear eddy-viscosity model*, Int. J. of Heat and Fluid Flow **18** (1997) pp. 15-28.

[12] A. D. D. Craik, *Nonlinear resonant instability in boundary layers*, J. Fluid Mech. **50** (1971), pp. 393-413.

[13] C. Dopazo , *Relaxation of initial probability density functions in the turbulent convection of scalar fields*, Phys. Fluids **22** (1979), pp. 20-30.

[14] M. E. Goldstein and L. S. Hultgren, *Nonlinear spatial evolution of an externally excited instability wave in a free shear layer*, J. Fluid Mech. **197** (1989), pp. 295.

[15] M. E. Goldstein, *Scattering of acoustic waves into Tollmien-Schlichting waves by small streamwise variations in surface geometry*, J. Fluid Mech. **154** (1985), pp. 509-529.

[16] T. Herbert, *Parabolized stability equations*, Annu. Rev. Fluid Mech **29** (1997), pp. 245-283.

[17] C. Hirsch, *Numerical computation of internal and external flows*, John Wiley, New York (1988).

[18] X. Huai, R. D. Joslin, and U. Piomelli, *Large-eddy simulation of transition to turbulence in boundary layers*, Theor. Comput. Fluid Dyn. **9** (1997), pp. 149-163.

[19] R. D. Joslin, C. L. Streett and C.-L. Chang, *Spatial direct numerical simulation of boundary-layer transition mechanisms: validation of PSE theory*, Theor. Comput. Fluid Dyn., **4** (1993), pp. 271-288.

[20] Yu. S. Kachanov, *Physical Mechanisms of Laminar Boundary-Layer Transition*, Annu. Rev. Fluid Mech. **26** (1994), pp. 411-482.

[21] Yu. S. Kachanov and V. Ya. Levchenko, *The resonant interaction of disturbances at laminar-turbulent transition in a boundary layer*, J. Fluid Mech. **138** (1984), pp. 209-247.

[22] L. Kleizer and T. A. Zang, *Numerical Simulation of Transition in Wall-Bounded Shear Flows*, Ann. Rev. Fluid Mech. **23** (1991), pp. 495-537.

[23] R. H. Kraichnan, *The structure of turbulence at very high Reynolds number*, J. Fluid Mech. **5** (1959), pp. 497-543.

[24] R. H. Kraichnan, *Decimated amplitude equations in turbulence dynamics*, in D. L. Dwoyer, M. Y. Hussaini, and R. G. Voigt (eds.), *Theoretical approaches to turbulence*, Springer-Verlag (1985).

[25] K. Kusunose and H. V. Cao, *Prediction of transition location for a 2-D Navier-Stokes solver for multi-element airfoil configurations*, AIAA Paper 94-2376, 1994.

[26] W. W. Liou and F. J. Liu, *Computational Modeling for the transitional flow over a multi-element airfoil*, AIAA Paper 2000-4322, 2000.

[27] M. R. Malik, *Boundary-Layer Transition Prediction Toolkit*, AIAA Paper 97-1904 (1997).

[28] R. R. Mankbadi, X. Wu, and S. S. Lee, *A critical-layer analysis of the resonant triad in boundary-layer transition: nonlinear interactions*, J. Fluid Mech. **256** (1993), pp. 85-106.

[29] R. W. Miksad, F. L. Jones, E. J. Powers, Y. C. Kim, and L. Khandra, *Amplitude and phase modulations during transition to turbulence*, J. Fluid Mech.

[30] P. A. Monkewitz, *Subharmonic resonance, pairing, and shredding in the mixing layer*, J. Fluid Mech. **188** (1988), pp. 223-252.

[31] S. B. Pope, *PDF methods for turbulent reactive flows*, Prog. Energy Combust. Sci. **11** (1985), pp. 119-192.

[32] C. D. Pruett, *Simulation of crossflow instability on a supersonic highly-swept wing*, NASA CR 198267 (1995).

[33] S. C. Reddy, P. J. Schmid, J. S. Baggett, and D. S. Hennigson, *Stability of streamwise streaks and transition thresholds*, J. Fluid Mech. (1998).

[34] E. Reshotko, *Boundary-Layer Stability and Transition*, Ann. Rev. Fluid Mech. bf 8 (1976), pp. 311-349.

[35] Ch. P. Ritz, E. J. Powers, R. W. Miksad, and R. S. Solis, *Nonlinear spectral dynamics of a transitioning flow*, Phys. Fluids **31** (1988), pp. 3577-3588.

[36] A. I. Ruban, *On the generation of Tollmien-Schlichting waves by sound*, Fluid Dyn. **19** (1985), pp. 709-716.

[37] R. Rubinstein, manuscript in preparation (2000).

[38] C. L. Rumsey, T. B. Gatski, S. X. Ying, and A. Bertelrud, *Prediction of High-Lift Flows Using Turbulent Closure Models*, Proc. 15th AIAA Applied Aerodynamics Conference, Atlanta, GA , AIAA 97-2260, June 23-25, (1997).

[39] W. S. Saric, V. V. Kozlov, and V. Ya. Levchenko, *Forced and unforced subharmonic resonance in boundary-layer transition*, AIAA-84-0007 (1984).

[40] B. A. Singer and S. P. G. Dinavahi, *Testing of Transition Region Models*, J. Fluids Eng. **114** (1992), pp. 73-79.

[41] A. M. O. Smith and N. Gamberoni, *Transition, pressure gradient and stability theory*, Douglas Aircraft Co., Report No. ES 26 388, El Segundo, CA (1956).

[42] P. R. Spalart, W-H. Jou, M. Strelets, and S. R. Allmaras, *Comments on the feasibility of LES for wings, and on a hybrid RANS/LES approach*, Advances in DNS/LES, *C. Liu and Z. Liu*, eds., Greyden Press, Columbus, OH, 1997.

[43] C. Speziale, *Turbulence modeling for time-dependent RANS and VLES: a review*, AIAA J., 36(2), 1998.

[44] H. W. Stock and W. Haase, *Navier-Stokes airfoil computations with e^N transition prediction including transitional flow regions*, AIAA J., 38(11), pp. 2059-2066, 2000.

[45] Y. B. Suzen and P. G. Huang, *Modeling of flow transition using an intermittency transport equation*, J. Fluids Engr., (June 2000).

[46] W. D. Thacker, C. E. Grosch, and T. B. Gatski, *Modeling the dynamics of ensemble-averaged linear disturbances in homogeneous shear flow*, Flow Turb. Comb. **63** (1999), pp. 39-58.

[47] F. Waleffe, *Homotopy of coherent states in wall-bounded shear flows*, Bull. Amer. Phys. Soc., (2000).

[48] J. WEILAND AND H. WILHELMSSON, *Coherent nonlinear interaction of waves in plasmas*, Pergamon (1977).

[49] D. C. WILCOX, *Turbulence modeling for CFD*, DCW Press, 1988.

[50] X. WU, S. J. LEIB, AND M. E. GOLDSTEIN, *On the nonlinear evolution of a pair of oblique Tollmien-Schlichting waves in boundary layers*, J. Fluid Mech. **340** (1997), pp. 361-394.

[51] K. YAMAMOTO, N. TAKAHASHI, AND T. KAMBE, *Direct numerical simulation of transition in plane Poiseuille flow*, Proceedings of the IUTAM Symposium on Geometry and Statistics of Turbulence, Hayama, Japan (1999).

[52] N. A. ZAVOL'SKII, V. P. RITOV, AND G. V. RYBUSHKINA, *Generation of Tollmien-Schlichting waves via scattering of acoustic and vortex perturbations in boundary layer on wavy surface*, J. Appl. Mech. Tech. Phys. (1983), pp. 79-86.

[53] M. B. ZELMAN AND I. I. MASLENNIKOVA, *Tollmien-Schlichting-wave resonant mechanism for subharmonic-type transition*, J. Fluid Mech. **252** (1993), 449-478.

[54] Z. ZHANG AND G. M. LILLEY, *A theoretical model of the coherent structure of the turbulent boundary layer in zero pressure gradient*, in Turbulent Shear Flows III, pp. 60-72, Springer-Verlag Berlin, (1982).

6. Appendix I: Finite volume integration of PDF evolution equation. In this Appendix, we present a brief description of the numerical method used to solve the PDF evolution equation Eq. (2.12) for a resonant triad.

We apply finite volume discretization, dividing the space of the independent variables r, r_3, θ into rectangular cells with side lengths $\Delta r, \Delta r_3, \Delta \theta$, where

$$(6.1) \qquad N(x \mid x_0, \sigma) = \frac{1}{\sqrt{2\pi\sigma^2}} e^{-(x-x_0)^2/2\sigma^2}$$

and assuming that P is constant in each cell. Let cell (i, j, k) be bounded by the planes $r = (i+1)\Delta r, r = i\Delta r, r_3 = (j+1)\Delta r_3, r_3 = j\Delta r_3, \theta = (k+1)\Delta\theta, \theta = k\Delta\theta$ Let $P_{i,j,k}$ denote the value of P in this cell, and let $\pi^r_{i,j,k}$ denote the value of P on the face on which $r = i\Delta r$, with analogous definitions for the values π^3 and π^θ. Integrating Eq. (2.12) over each cell produces the discrete equation

$$(6.2) \qquad P_{i,j,k}(t + \Delta t) = P_{i,j,k}(t) + \frac{\Delta t}{\Delta V_{i,j,k}} \{ \mathcal{F}^r_{i,j,k} + \mathcal{F}^3_{i,j,k} + \mathcal{F}^\theta_{i,j,k} \}$$

where

$$\mathcal{F}^r_{i,j,k} = \int dr \, \frac{\partial}{\partial r}(F_r P)$$
$$= F_r((i+1)\Delta r, j\Delta r_3, k\Delta\theta)\pi^r_{i+1,j,k} - F_r(i\Delta r, j\Delta r_3, k\Delta\theta)\pi^r_{i,j,k}$$
$$\mathcal{F}^3_{i,j,k} = \int dr_3 \, \frac{\partial}{\partial r_3}(F_3 P)$$
$$= F_3(i\Delta r, (j+1)\Delta r_3, k\Delta\theta)\pi^3_{i,j+1,k} - F_3(i\Delta r, j\Delta r_3, k\Delta\theta)\pi^3_{i,j,k}$$
$$\mathcal{F}^\theta_{i,j,k} = \int d\theta \, \frac{\partial}{\partial \theta}(F_\theta P)$$
$$(6.3) \qquad = F_\theta(i\Delta r, j\Delta r_3, (k+1)\Delta\theta)\pi^\theta_{i,j,k+1} - F_\theta(i\Delta r, j\Delta r_3, k\Delta\theta)\pi^\theta_{i,j,k}.$$

The assumption that P is constant in each cell implies that the fluxes $\mathcal{F}$ can be evaluated exactly, but the problem remains to evaluate the values on the faces π by interpolating the values of P in each cell. The

most obvious procedure of averaging the values of P across each face:

$$\pi_{i,j,k}^r = \frac{1}{2}[P_{i,j,k} + P_{i-1,j,k}]$$

$$\pi_{i,j,k}^3 = \frac{1}{2}[P_{i,j,k} + P_{i,j-1,k}]$$

(6.4)
$$\pi_{i,j,k}^\theta = \frac{1}{2}[P_{i,j,k} + P_{i,j,k-1}]$$

is well-known to be unstable [17]. A stable scheme results from the "upwind" method

(6.5)
$$\pi_{i,j,k}^r = \begin{cases} P(i,j,k) & \text{if } F_r(i,j,k) > 0 \\ P(i-1,j,k) & \text{if } F_r(i,j,k) < 0 \end{cases}$$

with analogous definitions for π^3 and π^θ, in which the value of π is the value of P at the cell into which the corresponding flux $\mathcal{F}$ points.

The accuracy of the computation degrades quickly if there is a probability flux across the boundaries of the region of integration. Since the amplitude distributions spread out, the region of integration must increase to prevent any loss of total probability. To maintain the total probability, the box sizes are rescaled at each time-step so that a fixed number of boxes always contain all but a small specified amount of the total probability. The rescaling is done on the basis of the standard deviations of the marginal distributions $P(r)$ and $P(r_3)$. Strictly speaking, rescaling based on the standard deviation is accurate only for Gaussian distributions, for which the region from about -4.5σ to $+4.5\sigma$ contains almost all of the probability; however, the calculations showed that this simple procedure was satisfactory in practice.

To implement this variable box-size, the governing equation is modified as follows: define the rescaled variables

$$r = \sigma_r x + m$$

(6.6)
$$r_3 = \sigma_3 x_3 + m_3.$$

Note that since the problem is periodic in θ, rescaling of θ is not possible. Instead of Eq. (2.12) we solve the modified equation

(6.7)
$$\frac{\partial \hat{P}}{\partial t} + \frac{1}{\sigma}\frac{\partial}{\partial x}\left([(F_r - \dot{\sigma}x - \dot{m})\hat{P}]\right) + \frac{1}{\sigma_3}\frac{\partial}{\partial x_3}\left([(F_3 - \dot{\sigma}_3 x_3 - \dot{m}_3)\hat{P}]\right) + \frac{\partial}{\partial\theta}(F_\theta\hat{P}) = 0$$

where the fluxes F_r, F_3, F_θ are the same as the fluxes in Eq. (2.6) and

$$\dot{m} = \int F_r\hat{P}dV$$

$$\dot{m}_3 = \int F_3\hat{P}dV$$

$$\dot{\sigma} = \int xF_r\hat{P}dV$$

(6.8)
$$\dot{\sigma}_3 = \int x_3 F_3\hat{P}dV.$$

For parametric excitation, the governing equation Eq. (2.12) is modified by altering the flux terms to

$$F_r = rr_3\cos\theta + \tilde{\sigma}r$$

$$F_3 = \sigma r_3$$

(6.9)
$$F_\theta = -2r_3\sin\theta$$

with the second modification Eq. (6.8) for rescaling, but otherwise, the numerical integration method is unchanged.

7. Appendix II: Results for inhomogeneous Gaussian random fields. In this Appendix, we derive some results used to formulate the conditionally Gaussian closure for PDF evolution equations.

For an inhomogeneous Gaussian random vector field $\psi_i(x)$, introduce the statistics

$$a_i(x) = \langle \psi_i(x) \rangle$$
$$r_{ij}(y,x) = \langle \psi_i(y)\psi_j(x) \rangle$$
$$\mathsf{C}_{ij}(y,x) = \langle \psi_i(y) \rangle \langle \psi_j(x) \rangle - \langle \psi_i(y)\psi_j(x) \rangle$$
$$\text{(7.1)} \qquad = -\langle [\psi_j(y) - \langle \psi_j(y) \rangle][\psi_i(x) - \langle \psi_i(x) \rangle] \rangle.$$

Note that the covariance matrix C is nonsingular.

Conditional expectations are found from the linear regression equation which is exact for Gaussian random fields

$$\text{(7.2)} \qquad \langle \psi_i(y) \mid \psi_1(x) \cdots \psi_n(x) \rangle = a_i(y) + \mathsf{C}_{im}(y,x)\mathsf{C}_{mj}(x,x)^{-1}[\psi_j(x) - a_j(x)]$$

Consequently, conditional expectations of derivatives are given by

$$\left\langle \frac{\partial \psi_i}{\partial x}(x) \mid \psi_1(x) \cdots \psi_n(x) \right\rangle = a_i'(x) + \frac{\partial \mathsf{C}_{im}}{\partial y}(y,x) \mid_{y=x} \mathsf{C}_{mj}(x,x)^{-1}[\psi_j(x) - a_j(x)]$$
$$\text{(7.3)} \qquad \left\langle \frac{\partial^2 \psi_i}{\partial x^2}(x) \mid \psi_1(x) \cdots \psi_n(x) \right\rangle = a_i''(x) + \frac{\partial^2 \mathsf{C}_{im}}{\partial y^2}(y,x) \mid_{y=x} \mathsf{C}_{mj}(x,x)^{-1}[\psi_j(x) - a_j(x)]$$

where we can substitute

$$\text{(7.4)} \qquad \frac{\partial^2}{\partial y^2}\mathsf{C}_{ij}(y,x) \mid_{y=x} = \langle a_i''(x) \rangle \langle a_j(x) \rangle - \frac{\partial}{\partial x}\left\langle \frac{\partial \psi_i(x)}{\partial x}\psi_j(x) \right\rangle + \left\langle \frac{\partial \psi_i(x)}{\partial x}\frac{\partial \psi_j(x)}{\partial x} \right\rangle$$

so that multiplication by the viscous term V leads to a dissipative correlation.